JOURNAL OF Materials CHEMISTRY
Feature Article

Electrically conductive oxide aerogels: new materials in electrochemistry

Debra R. Rolison[a] **and Bruce Dunn**[b]

[a]*Surface Chemistry Branch, Code 6170, Naval Research Laboratory, Washington DC 20375-5342, USA. E-mail: rolison@nrl.navy.mil*
[b]*Department of Materials Science and Engineering, UCLA, Los Angeles CA 90095-1595, USA. E-mail: bdunn@ucla.edu*

Received 19th September 2000, Accepted 22nd November 2000
First published as an Advance Article on the web 19th February 2001

Aerogels, which are nanoscale mesoporous materials of low density and high surface area, have been well studied as thermal insulators, heterogeneous catalysts, and novel particle or radiation detectors. Now, electrically conducting oxide aerogels are being explored as new materials in electrochemistry and for their innate ability to amplify the nature of the surfaces of technologically relevant conducting oxides in batteries, ultracapacitors, and fuel cells. Recent results are reviewed in which the mixed electron- and cation-conducting transition metal oxides of vanadium, molybdenum, ruthenium, and manganese have been prepared as low density, highly porous, and high surface area aerogels and then studied as charge-storage electrode materials. These materials challenge the standard ways in which electrochemically active oxides are conceived, studied, and used.

Introduction

What is an aerogel? And why are aerogels materials of interest?

We consider aerogels to be composites of being and nothingness[1,2] (with few or no apologies to Sartre[3]) because they are mesoporous materials in which nanometer-scale solid domains (the "being") are networked through a continuous, highly porous volume of free space (the "nothingness"), as depicted in Fig. 1.[4,5] This combination of being and nothingness is key to the unique properties of aerogels because a number of important physical attributes are assembled into one architecture. These properties include: *(1)* high surface area; *(2)* stabilization of nanoscale matter to coalescence or agglomeration; *(3)* low (and controllable) densities (the ratio of being to nothingness); and *(4)* accessibility of molecular reactants to the nanoscale domains throughout the aerogel *via* rapid mass transport through the continuous volume of mesopores (pores sized at >2 nm).

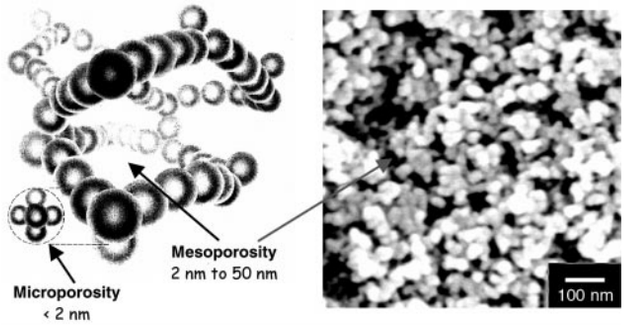

Fig. 1 (Left) Representation of the architectural being and nothingness of an aerogel illustrating the innate nanoscopic character of the solid and pore components of these low density, highly porous, sol–gel-derived materials (adapted from ref. 4). (Right) High resolution scanning electron micrograph showing the general features seen for silica (and silica-based composite) aerogels: 10 to 20 nm diameter silica domains networked through mesoporous space [(ref. 5) Reprinted with permission from M. L. Anderson, R. M. Stroud, C. A. Morris, C. I. Merzbacher and D. R. Rolison, *Adv. Eng. Mater.*, 2000, **2**, 481. Copyright [2000] Wiley-VCH].

This review is directed at the prospect and promise that aerogels offer as a new direction in electrochemical materials. Aerogels have been explored, with a focus on insulating oxide materials, for a wide range of applications in physics, engineering, and catalysis.[6] All the attributes that make aerogels appealing materials in these fields also offer potential contributions to electrochemistry provided the solid network is electrically conducting, *i.e.*, when it can transport electrons and/or ions. To explore the possibilities for aerogels in electrochemical applications, a context will first be created based on the wealth of information available on the physical and chemical properties (and applications) of aerogels in physics, engineering, and catalysis. We will then describe the recent research on aerogels as new materials in fuel cells, batteries, supercapacitors, and electrocatalysis.

We also wish to emphasize in our discussion that aerogels offer another contribution to electrochemical science and technology—one beyond that of providing new materials or architectures. Because aerogels innately magnify the surface-to-volume fraction of a material, aerogels are also tools that amplify (and thereby offer a new way to explore and understand) the critical phase of any electrochemical system: the interface.

History and background

The widespread interest in aerogels arises not only from their unique microstructural features of low density and high surface area but also because these morphologies can be obtained for a variety of chemical compositions. The first aerogels were prepared in the 1930s by Kistler who used supercritical drying (SCD) to replace the liquid phase in a wet gel with air.[7] Above the critical point, the liquid phase no longer exists and formation of liquid–vapor interfaces—and the capillary forces that subsequently collapse the drying gel to a xerogel—are avoided. Removing the pore liquid without collapsing the microstructure preserves both the solid and porous networks so that the resulting solid—an aerogel—retains the high porosity, low density and high surface area of the wet gel. Kistler immediately recognized that the synthesis of aerogels was a property of gels in general and not restricted to a few systems.[7] He and his co-workers rapidly explored the application of

aerogels as catalysts and catalyst supports[8] and determined that silica aerogels exhibit extremely low thermal conductivity.[9]

The Kistler method for preparing aerogels is cumbersome and for nearly 30 years these materials went largely uninvestigated. An important development occurred in the 1960s when Teichner and Nicolaon prepared aerogels by what is now commonly known as the sol–gel process.[10] This technique eliminated the time-consuming salt removal and solvent-exchange steps inherent to the Kistler method and enabled aerogels to be prepared in hours rather than days. Moreover, the sol–gel method readily extends aerogel chemistry to transition metal oxides, to binary and ternary oxide compositions, to metal/metal oxide systems and even to organic/inorganic hybrid materials. To some degree the development of aerogels as novel materials parallels the emergence of sol–gel science and technology since the 1980s[11] and it is evident that aerogels will continue to benefit from the continued interest in, and variations on, sol–gel synthetic approaches.

Aerogel synthesis

The synthesis of oxides by sol–gel methods has been well reviewed,[11,12] as sol–gel chemistry is one of several liquid-phase (*i.e.*, soft or *chimie douce*[13]) methods to prepare inorganic materials.[14] Focused reviews on the adaptation of sol–gel processing for aerogels have appeared.[15–18] Thus, only a brief overview of pertinent synthetic issues is presented here.

Three routes are currently used to prepare sol–gel materials and they are distinguished by the nature of the precursor: an inorganic salt (in aqueous solution), an aggregate of colloidal particles in a solvent, or a network-forming species in an organic or aqueous solution. The last route has emerged as the most widely traveled because network-formers can be modified to control the resulting chemistry and processing of the gel, and ultimately its morphology. Among the different network-forming precursors, metal alkoxides have clearly become the most important ones, although metal β-diketonates and metal carboxylates are also used. The sol–gel route involving metal alkoxides ($M(OR)_n$, where M is Al, Si, Ti, V, Cr, Mo, W, *etc.*, and OR is an alkoxy functionality[19]), may be considered as a two-step inorganic polymerization.[12] Initiation occurs *via* hydrolysis of alkoxy ligands to yield an alcohol (ROH) and, as new reactants, hydroxylated metal centers (M–OH):

$$M(OR)_n + H_2O \rightarrow [M(OR)_{n-1}(OH)] + ROH \quad (1)$$

Three-dimensional propagation then occurs as the hydroxylated species condense to form oxypolymers. Polycondensation involves an oxylation reaction which creates oxygen bridges and expels XOH species as follows:

$$M{-}OH + M{-}OX \rightarrow M{-}O{-}M + XOH \quad (X = H \text{ or } R) \quad (2)$$

The nature of the inorganic network depends upon the relative rates of hydrolysis and condensation. Under synthetic conditions where hydrolysis is favored and condensation is the rate-determining step, small hydroxylated oligomers predominate ultimately yielding polymer-like gels with relatively small pores. When high condensation rates are favored, the resulting gel network consists of interconnected colloidal particles and large pores. These colloidal gels are generally preferred for aerogels because the large pores make it easier to remove the pore liquid during supercritical drying.[18]

The chemical reactivity of metal alkoxides $M(OR)_n$ towards hydrolysis and condensation mainly depends on the nature of the metal atom—both its electrophilicity and its ability to undergo an increase in coordination number.[12] For example, silicon alkoxide $Si(OR)_4$ precursors have a low electrophilicity and their coordination number is stable because the silicon precursor and product oxide have the same coordination number ($N = 4$). Thus, hydrolysis of $Si(OR)_4$ is slow and the rates of the polymerization reactions of these alkoxides are mainly controlled by acid or base catalysis.

The sol–gel chemistry of non-silicate systems is not as easily controlled, especially for metal alkoxides in which the transition metal centers are highly electrophilic and exhibit several coordination states.[12] Most transition metal alkoxides are so reactive that precipitation occurs as soon as water is added. One means of moderating the reaction rates is to chemically modify the precursor.[20] Since transition metal alkoxides react with nucleophilic reagents, they can be modified by using complexing ligands HOA (*e.g.*, OA = acetylacetonate, acetate):

$$M(OR)_n + mAOH \rightarrow [M(OR)_{n-m}(OA)_m] + mROH \quad (3)$$

In this case the alkoxy groups (OR) are replaced by new ligands (OA) that are more stable to hydrolysis. Thus, the alkoxy ligands are rather quickly removed upon hydrolysis while chelating ligands act as termination agents that limit condensation reactions.[21]

The manner in which the liquid phase is removed from a wet gel determines whether the dried material is a highly porous aerogel or a more dense xerogel (Fig. 2). The latter is characterized by collapse of the wet gel's structure as the pore liquid evaporates. If the network is compliant, the gel deforms from the capillary forces generated by the liquid phase as it recedes into the body of the gel. The capillary pressure (P_c) is related to the liquid–vapor interfacial energy of the solvent (γ_{lv}), the liquid–solid contact angle (θ), and the surface-to-volume ratio of the pores (S_p/V_p);[22]

$$P_c = \gamma_{lv} \cos(\theta) \left(\frac{S_p}{V_p}\right) \quad (4)$$

The S_p/V_p ratio can be re-written in terms of the bulk density[23] of the gel (ρ_b), its skeletal density (ρ_s, which approaches that of the dense form of the oxide) and the specific surface area, S;

$$\left(\frac{S_p}{V_p}\right) = \frac{S\rho_b}{1-\rho} \quad (5)$$

where ρ represents the fraction of matter in the gel volume (ρ_b/ρ_s). For aerogels (where $\rho_b < \rho_s$) ρ is usually less than 0.1.

The capillary pressure can now be expressed in terms of more easily measured parameters:

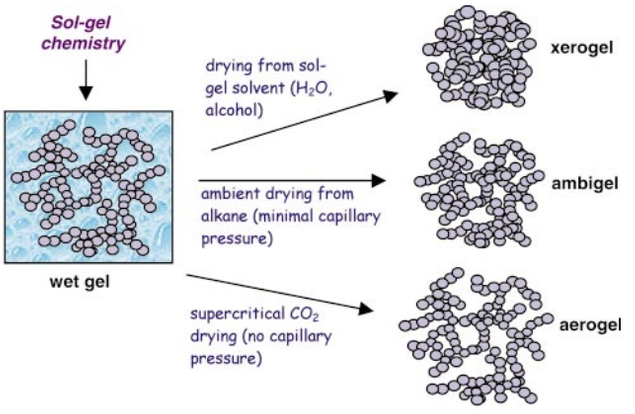

Fig. 2 The method used to extract the pore fluid from a wet gel creates a dry solid with variable porosity: strong capillary forces create a xerogel, weak capillary forces create an ambigel, and zero capillary force creates an aerogel that nominally retains the low density framework of the wet gel.

$$P_c = \gamma_{lv} \cos(\theta) \left(\frac{S \rho_b}{1 - \rho} \right) \quad (6)$$

The issues associated with capillary pressure and the shrinkage that results upon drying have been well developed as there is considerable interest in obtaining crack-free xerogels for a variety of applications.[11]

Both supercritical and ambient-pressure routes can produce aerogels.[24] The SCD methods "preserve" the porosity of the wet gel by bringing the solvent phase into its supercritical state, where no liquid–vapor interfaces exist, so that capillary stresses never develop. Researchers distinguish between high temperature and low temperature SCD.[15] The former, pioneered by Kistler, removes the alcohols produced as by-products during the sol–gel process. But the typical SCD conditions for alcohols—250 °C at 5 to 8 MPa—not only create a safety concern but also accelerate gel-aging processes leading to materials with little microporosity and lower surface area. The low temperature process introduced by Hunt and co-workers[25] is adapted from the biology community[26] in which liquid CO_2 is taken supercritical at similar pressure levels ($\sim$8 MPa) but at temperatures just above room temperature (30–40 °C). Liquid CO_2, however, is poorly miscible with most solvents, so intermediate solvent exchange of the pore liquid with a more CO_2(l)-miscible solvent (*e.g.*, acetone or amyl acetate) is generally necessary. The advantages and disadvantages for the two SCD methods have been well discussed in the literature.[15]

Ambient-pressure methods for preparing aerogels are just emerging. These approaches offer great promise to lower aerogel production costs and thus represent an important consideration for the future development of these materials. Ambient-pressure methods for silica aerogels include both surface modification[27–29] and network strengthening.[30–32] The former involves the use of organic surface treatments in which terminal silanols (Si–OH) are replaced by nonreactive groups *via* silylation[27,28] or esterification.[29] These surface modifications inhibit condensation reactions (conversion of Si–OH centers to Si–O–Si, which locks in structural collapse by sealing compressed pores shut), so that the porous network can "spring back" to nearly the original volume of the wet gel. Both bulk (monolithic) and thin film silica aerogels have been prepared by the spring-back method.[27,28]

Network strengthening involves either aging the wet gel in its mother liquor (including thermal treatments in water[30]) or soaking it in a silicon alkoxide during the washing and aging steps.[31,32] Terminal silanols on the silica gel react with Si–OR moieties to coarsen the gel network and increase the network's resistance to collapse from the capillary forces generated during ambient-pressure drying. Low density silica aerogels with specific surface areas of $\sim$700 $m^2\ g^{-1}$ have been reported.[31,32] In a recent report, an alternative to these methods showed that aerogel-like materials were produced by aging silica gel for three weeks in its dialkylimidazolium-based mother liquor, followed by refluxing in acetonitrile to extract the ionic liquid and ambient-pressure drying to remove the acetonitrile.[33]

Ambient-pressure methods can also be realized by using pore solvents with low surface tension,[32,34] but only recently were such solvents more thoroughly examined and extended to compositions other than silica.[35] In this approach the pore liquid is exchanged with low surface tension, nonpolar solvents prior to ambient-pressure drying (Fig. 2). The method should be applicable to a wide variety of systems, as indicated from results obtained with vanadium oxide,[35,36] molybdenum oxide,[35] and manganese oxide.[37,38] The ambient-dried transition metal oxides (hereby christened ambigels) are somewhat less porous than the corresponding SCD materials (80% *vs.* 90%), but exhibit comparable surface areas and pore volumes.

Materials systems and applications

The development of aerogel materials has been closely coupled to two of their most prominent physical properties: high surface area and low thermal conductivity. The former is of interest in catalysis and has led researchers to investigate a wide range of compositions. Low thermal conductivity is a property of aerogels in general,[6] but has been studied extensively in silicate systems because of the considerable understanding of the sol–gel process for silicates and the range of their potential applications.

Aerogel catalysts. Aerogels have been investigated as heterogeneous catalysts since their inception in the 1930s.[7] Aerogels offer more active sites per gram for gas/solid interactions than do more dense materials. Sol–gel chemistry and processing allow specific compositions to be developed with a highly porous morphology, so that the solid network can be tailored to the specific catalytic reaction while the mesoporous network serves as the equivalent of a superhighway for molecular transport. Just as with zeolites,[39] the area of the "external" surface of an aerogel is relatively small compared to its "internal" surface area.[15] Unlike zeolites, which are *microporous*, crystalline solids,[39] the continuous *mesoporous* network of aerogels facilitates the flux of reactant molecules that access the catalytically active "internal surface" area. The rates of catalytic reactions that are transport-limited rather than kinetically limited would be improved by what an aerogel innately provides: ready mass transport of reactants to an increased area of catalytic surface.

Much of the work on aerogel catalysts[15,17,40] draws on the many metal or metal oxide (MOx)-based catalysts that have already been studied on traditional oxide supports.[41] In addition to high surface area and mesoporosity, other benefits of the sol–gel method for preparing catalysts include liquid-phase syntheses so that mixing on the molecular scale can give rise to homogeneous products; the ability to adapt the physical properties of aerogels (density, particle size, mechanical properties) to the requirements of the catalytic application and reactor type; and the moderate temperatures of sol–gel chemistry and processing, which allow preparation of amorphous or metastable catalysts.

The range of aerogel catalysts is extensive[15,17,18,40] and includes a variety of single component, binary and ternary oxide systems along with M/MOx compositions supported on aerogels. Similarly, a wide range of catalytic reactions have been studied on aerogels, such as hydrogenation and dehydrogenation reactions, hydrodesulfurization, partial oxidation, ammoxidation, nitroxidation, and selective reduction of NO.[15,17,18,40] Aerogel catalysts as prepared by high *vs.* low temperature SCD may differ significantly, not only in terms of surface area[40] but also in their fundamental behavior. High temperature SCD preparation of aerogels can induce crystallization of the oxide,[17] which may or may not be desirable for the specific catalytic reaction. Furthermore, the reducing properties of alcohols at high temperature and pressure can lead to *in-situ* reduction of metal ions or metal oxides. M/MOx-impregnated aerogels dried *via* high temperature SCD can exhibit high catalytic activity without thermal pre-treatment,[15,17] as first seen for Ni/NiO- or Pt/PtO-impregnated SiO_2[42] and subsequently extended to other metals and oxide aerogels, *e.g.*, Pd/Al_2O_3.[43] In contrast, low temperature SCD-derived aerogels typically require thermal activation prior to their use as catalysts.[15]

If the number of reactant-accessible catalytic sites per gram is improved, the number of molecules reacted (turnover number, TON) per unit time (turnover frequency) increases, which improves the efficiency of the reaction. However, the mechanism of the catalytic reaction effectively does not change if surface-area normalized TONs for the aerogel catalyst are

comparable to those for its standard heterogeneous catalyst relative. Comparable surface-area-normalized rates indicate that the rate-determining step and the physicochemical nature of the reaction environment are unaffected. Many examples of this comparability are found in the literature.[15,17,40] A more interesting (and desired) divergence occurs when the aerogel-based catalyst is more active than its standard heterogeneous catalyst relative, even after normalizing for surface area differences.

An interesting feature of aerogel catalysts is the inherent disorder present in these materials. Although heterogeneous catalysis is modeled using calculations on and experiments with well-defined single-crystal metal or metal-oxide surfaces, such models are acknowledged as reference points for the practical systems.[44] Heterogeneous catalysts are, in general, non-smooth, high surface area, nanoscale materials. However, should the catalytic activity derive from a disordered structure, preparations that enhance amorphous or defective, rather than crystalline, components of the catalyst are advantageous. Teichner reports an example in which the less-ordered form of an iron oxide catalyst, as realized by the aerogel route, leads to improved surface area-normalized TONs for Fischer–Tropsch chemistry to synthesize hydrocarbons:[45]

$$3H_2 + CO \xrightarrow[\substack{Fe_2O_3\|Al_2O_3\\ aerogel}]{} H_2O + CH_4 \qquad (7)$$

In a recent study of alkene isomerizations and dimerizations, Sun and Klabunde demonstrated that the activity of sol–gel-processed MgO aerogel catalyst greatly exceeded that of more conventional MgO forms.[46] Potassium-promoted MgO aerogel was shown to have a higher base strength (as determined using indicator dyes), which derived from stronger and higher numbers of base sites than exist in the non-aerogel MgO materials. Further, the catalytic activity correlated with the expected surface concentration of edge/corner sites of poly-crystalline MgO and the nanoscale form of the aerogel maximizes the number of such sites.

Despite the obvious advantages aerogels bring to catalysis as either the primary catalyst or the catalyst support, the transition of these materials into practical catalytic processes appears to be limited, at least as reported in the open literature. Ko discusses how one cycle of hydrotreating deleteriously lowered the surface area of a Ni–Mo/TiO_2–ZrO_2 aerogel catalyst.[40,47] The origin of the effect, collapse of micropores in the nanoscale domains of the mixed-oxide aerogel, underscores the importance of stabilizing the aerogel microstructure.

One approach to stabilize the solid network of an aerogel to the chemistries, temperatures, and pressures implicit in heterogeneous catalysis is to start with partially densified aerogels. Fricke and co-workers have shown that the density of SiO_2 aerogels can be monotonically increased by calcining SCD-prepared aerogels above 800 °C.[48] The degree of densification, which can be as modest an increase as 0.15 to 0.25 g cm^{-3} for silica (with a bulk density of $\sim$2.2 g cm^{-3}) is controlled by the time spent at elevated temperatures. Partially densified aerogels have improved mechanical integrity,[48–50] and can withstand re-exposure to liquids and ambient drying without cracking[50] and without loss of surface area or pore volume upon ambient evaporation of the filling liquid.[51] Partially densified aerogels have been proposed as hosts to synthesize multicomponent materials by infusion of liquid precursors into the open volume of the aerogel:[50] such an approach should offer a more durable material for heterogeneous catalysis.

Aerogel reactants. The high surface area and enormous mesoporous volume of aerogels offer opportunities for chemical reactivity other than in catalysis. A good example is one where the aerogel oxide acts as a stoichiometric chemical reactant.[52] Klabunde and co-workers have explored MgO and CaO aerogels for base-catalyzed decomposition of organic molecules that are environmental hazards, particularly chlorinated[53–55] and fluorinated[56] organic molecules and organophosphonates.[57] Calcium oxide acts as a reagent for the thermal destruction of CCl_4 to form non-toxic products:

$$CCl_4 + 2CaO \xrightarrow{\Delta} CO_2 + 2CaCl_2 \qquad (8)$$

Klabunde and co-workers found that CaO aerogels have higher decomposition efficiencies than other forms of nanoscale CaO. The higher performance is attributed to both higher surface area (relative to other fine powders of MgO or CaO) and higher surface reactivity.[52,55] These highly active sites are due to a large number of three- and four-coordinate ions with a higher Lewis basicity, caused by the increased number of corner, edge and defect sites, when compared to standard MgO samples,[58] as shown in Fig. 3. The decomposition of CCl_4 on CaO aerogel is so rapid at 700 K that it cannot be followed spectroscopically.[52] Modifying MgO or CaO aerogel cores with shells of metal oxides, including Fe_2O_3 and V_2O_5, improves the decomposition capacity so that essentially stoichiometric reaction of the solid base with CCl_4 or 1,3-dichlorobenzene occurs. The metal oxide supported on the aerogel seems to act as a chloride ion shuttle between the organic and the MgO aerogel core.[59]

Applications of aerogels based on physical properties. Silica aerogels constitute a model aerogel system[11,60] because the relationships have been detailed among sol–gel chemistry, the resulting aerogel microstructure, and the effect on physical properties.[16] In particular, the ability to obtain a highly porous microstructure with controlled pore size[61,62] is of considerable importance for the physical applications of aerogels as discussed below.

Aerogels are among the best thermal insulators available on the planet[63] due to their extremely low thermal conductivities. Although all aerogels possess this property to some degree, silica aerogels have received the most attention.[64] In addition to being non-flammable and inert, the ability to make silica aerogels as transparent thermal insulators offers a unique opportunity in which the material effectively transmits solar light, but strongly blocks thermal infrared radiation.[65] Another promising application area is in non-evacuated thermal insulation systems, where aerogels perform significantly better than CFC-blown foams.[16] In this case, transparency is not important and the radiative thermal conductivity can be reduced significantly by the addition of opacifiers such as

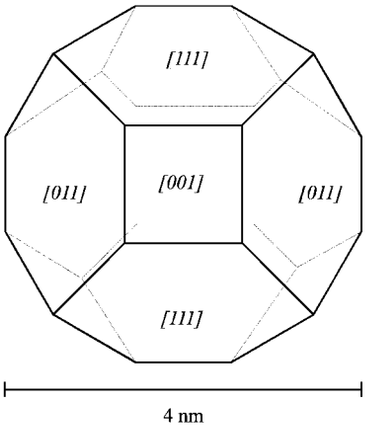

Fig. 3 Idealized representation of a 4 nm crystallite of aerogel-produced MgO.[58] CaO and MgO, in their aerogel-produced form, lead to higher activity for thermal decomposition of environmentally proscribed organic compounds containing chlorine, fluorine, phosphorus, or sulfur than nanocrystalline CaO or MgO prepared by other approaches.

carbon soot or TiO_2.[66] In general, the thermal insulation opportunities for aerogels are extensive; the key features that limit their commercialization for this purpose and others are cost and related manufacturing issues. Smith *et al.* have pointed out that only high-value products can justify the exorbitant expense of introducing and removing liquids, multiple times—a processing component currently integral to the production of aerogels.[67]

The porous morphology of aerogels leads to certain novel properties in areas other than those based on thermal conductivity.[68] In acoustics, for example, the extremely low sound velocity in SiO_2 aerogels is useful for impedance-matching applications in ultrasonic sensor systems.[69] Silica aerogels are widely used for Cerenkov detectors because they offer a critical range of low refractive index values (1.007 to 1.024) otherwise difficult to achieve except with compressed gases, which eases detector fabrication.[16,70,71] Physicists have also used aerogels as the matrix to hold supercooled helium to study phase transitions,[72] including the superfluid transition in ^3He.[73] Another exotic application for aerogels is their use in the intact capture of cosmic dust particles (micrometeorites) traveling at hypervelocities (>3 km s^{-1}).[74] The porous morphology of the aerogel provides a thermally stable, inert medium to dissipate the kinetic energy of the speeding particle while its transparency enables the captured particle's final location to be directly observed. The effectiveness of aerogels as micrometeorite detectors has been demonstrated on several Space Shuttle missions and is the subject of the "Stardust" mission, launched on 7 February 1999, which is scheduled to parachute back to earth in 2004 for analysis of the collected comet dust.[75]

Another area where the highly porous morphology of aerogels is generating enormous interest is in microelectronics.[76] The opportunities here should have widespread impact because interlayer dielectrics (ILD) with dielectric constants less than that of dense silica ($\varepsilon \sim 4$) are critical for high speed devices.[77] As indicated in the Semiconductor Industry Association (SIA) "Roadmap", there is a vital need for a new generation of low dielectric constant materials in order to improve device performance as smaller feature sizes in integrated circuits are developed.[78] Silica aerogels represent one of the most promising of all materials for ILD because of their low dielectric constant ($\varepsilon < 2$), thermal and dimensional stability, and compatibility (*e.g.*, spin-on methods) with semiconductor processing. The development of silica aerogel films for ILD applications is well underway.[77]

Tailoring the properties of aerogels. In designing aerogels for specific physical and chemical applications, including electrochemistry, one key advantage resides in the variety of means available to modify the (wet and dry) gels chemically and thereby tailor the final properties of the modified aerogels. As seen in Fig. 4, chemical modification can be broached at multiple points in the creation of an aerogel, by: *(i)* modification of the sol–gel precursor; *(ii)* addition of a particulate phase during sol–gel formation; *(iii)* liquid-phase modification of the wet gel; *(iv)* gas-phase modification of the aerogel; and even *(v)* liquid-phase modification of an annealed or strengthened aerogel.

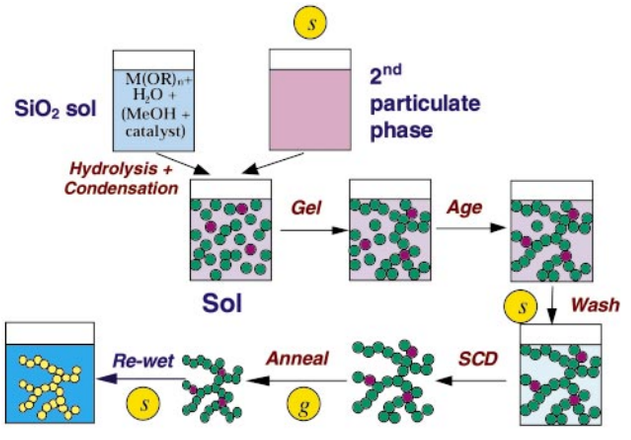

Fig. 4 Points during sol–gel chemistry and processing at which the sol, wet gel, supercritically dried gel (aerogel), or re-wetted aerogel may be chemically modified; s = solution, g = gas phase.

Several examples of aerogel design flexibility have been demonstrated to date. Catalysts based on the dispersion of metals on aerogel supports have been well investigated,[15,17,79] as have aerogels to which opacifiers are added to reduce thermal transport or that are heated at elevated temperatures to obtain partially densified aerogels.[48–50,66] Aerogels with new properties continue to be created. One recent development involves doping aerogels by gas-phase decomposition reactions.[80] This approach takes advantage of the open-pore network of the aerogel and appears adaptable to a wide range of organic and inorganic dopants derived from standard chemical vapor deposition precursors.[80–83] A related method of deposition uses a sub-0 °C decomposition of thermally sensitive metal-based precursors to modify the surfaces of partially densified silica aerogels.[51] The ability to fabricate conductive nanowires within silica aerogels by this approach is discussed later.

Another recent development is the synthesis of organic/inorganic hybrid aerogels.[84] The use of sol–gel methods to prepare a wide range of organic/inorganic xerogels has emerged rapidly over the past five years,[84,85] and it is evident that aerogels can benefit greatly from this existing work. Aerogels with improved hydrophobic character and elastic properties have already been reported;[84] hybrid aerogels with modified electrochemical properties are described later.

Enabling results for aerogels in electrochemical applications

The charge-transfer processes innate to electrochemistry require that sufficient quantities of ion charge must be established and moved. This demand means that most of electrochemical science occurs in media of high dielectric constant, and much of that in the liquid phase. Traditional applications for aerogels are "dry" as described previously and there has not been the need to consider the energetics of wetting, rather than the energetics of drying, the enormous quantity of nanoscopic surface. But, as we discuss in detail below, aerogel powders and films have already been studied in both aqueous and non-aqueous electrolytes, in which the solvents are such polar liquids as water, acetonitrile, propylene carbonate, and dimethylformamide. Extensive structural studies have yet to be done to verify that exposure to liquid electrolyte does not catastrophically collapse an aerogel's pore architecture upon immersion. However, available results indicate that when the density of the aerogel is not ultralow, immersion even into water will not destroy an aerogel's porous network.

Merzbacher *et al.* used small-angle neutron scattering (SANS) to characterize the structural integrity of a silica aerogel ($\rho \sim 0.12$) as a function of refilling the micropores and mesopores with a high surface tension liquid.[86] Within the ability of the neutron experiment to discern structural change, no damage on the length scale of the primary features of the aerogel's architecture ($\sim$2–100 nm) was observed upon replacing the air in the aerogel's pores with D_2O, Fig. 5.[86,87] SANS studies also show that an electrically conductive mixed-oxide aerogel of RuO_2–TiO_2 ($\sim$12% dense relative to the bulk density of the mixture) can be immersed in H_2O : D_2O mixtures without damage to the aerogel.[88]

Another enabling attribute required of aerogels as electro-

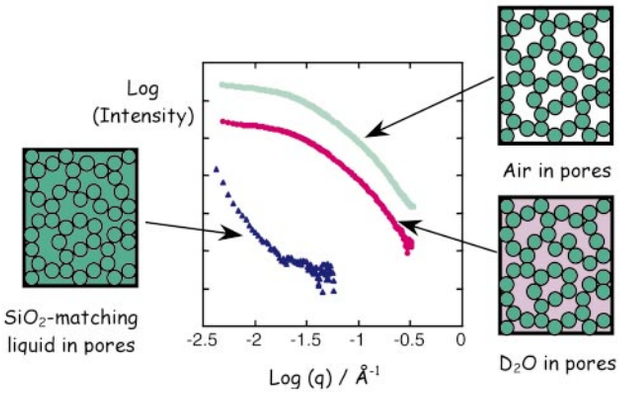

Fig. 5 Small-angle neutron scattering from silica aerogels before and after filling the pores with a high surface tension liquid (D_2O) and a contrast-matching liquid chosen to null out the scattering from the silica [(data taken from ref. 86) Reprinted from *J. Non-Cryst. Solids*, 224, C. I. Merzbacher, J. G. Barker, K. E. Swider and D. R. Rolison, "Effect of re-wetting on silica aerogel structure: a SANS study", 92–96. Copyright [1998], with permission from Elsevier Science].

chemical objects is process compatibility. Many practical electrodes, such as those present in batteries and fuel cells, are composite structures containing the true electrochemical actor (*e.g.*, the active material in a battery; the electrocatalyst in a fuel cell) plus other components that optimize the performance of the practical electrode (Fig. 6a). These additional materials can include conducting carbon blacks, polymeric binders, and additives that affect shape changes in battery electrodes or improve proton conductivity in fuel-cell electrodes.[89] The composite nature of such electrode structures requires that the aerogel, most likely in use as a powder, be durable in the face of grinding or pressing and that it exhibit some stability to heating (*e.g.*, as necessary to remove dispersion solvents or to take polymeric binders above their glass-transition temperatures).

Swider *et al.* have shown that the BET (Brunauer–Emmett–Teller) surface area of RuO_2–TiO_2 aerogel (at $\sim 85\ m^2\ g^{-1}$) does not decrease when the monolithic form is pulverized to powder or pressed (at hand pressure) into a free-standing pellet, and even appears to increase slightly.[1] In electrochemistry, current scales with the surface area of the electrified interface,[90] so it is desirable that any mechanical processing involved in fabricating an electrode structure does not diminish any surface area capable of being electrified. Richards *et al.* have also reported that the high specific surface area of aerogel-produced MgO is retained (and, again, slightly increases) when the powder is pressed at low-to-medium pressure into pellets.[91] Because the feature size of the solid phase in aerogels is on the order of 10 nm, it is reasonable that such fine domains are not damaged during moderate mechanical treatments. In agreement with that assessment, SANS indicates that the scattering curves for monolithic silica aerogel and powder derived from it are identical until the length scale of the powdered particulate is reached.[86]

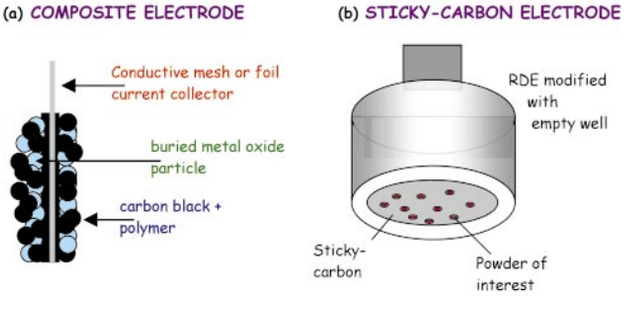

Fig. 6 (a) Practical electrode structure in which the electrochemically active powder is mixed with conductive carbon powder and polymer binders in order to cast (from solvent) or press a conductive composite. (b) Electroanalytical electrode structure in which the electrically conducting powder is studied without exposure to other chemicals by hand-pressing onto the surface of a "sticky carbon" rotating disk electrode (RDE) made of a carbon-wax composite.

Another important attribute of aerogels for electrochemical applications is how the nanoscale matter of an aerogel resists both coarsening and agglomeration. In electrochemistry this resistance translates to stabilizing the electroactive surface area defined by the walls of the mesopores. The aerogel architecture inherently lowers the number of near-neighbor domains—and their mobility—so although these materials can coarsen under temperature and pressure (as dependent on the energetics of the specific oxide), their ability to do so is lessened because there simply is less matter nearby to coalesce. Agglomeration is suppressed because the particles comprising the solid fraction of an aerogel are held in a rigid framework.

Synthesis and properties of conductive oxide aerogels

Why should one go to the extra processing necessary to create an electrode material from nanoscale mesoporous solids? Primarily because of the ability we now have to control—on the nanoscale—the arrangement of electroactive matter in space. This design and synthetic control permits exploration of how electrochemical processes are influenced by *(1)* minimized solid-state diffusion lengths; *(2)* effective mass transport of ions and solvent through the mesopores to the nanoscale, networked electrode material; and *(3)* amplification of the surface (and surface defect) character of the electroactive material.

We have chosen to focus this discussion just on the conductive oxides (Table 1) rather than include the other noted type of conductive aerogel, namely, carbon aerogels formed by pyrolysis of resorcinal–formaldehyde (or melamine–formaldehyde) polymeric aerogels.[92] Carbon aerogels join a large, properties-related class of highly porous carbons. They have already been studied as high surface area, porous electrodes, especially for applications in which charge (in the form of mobile, solution-phase ions) is stored at electrified interfaces either for energy storage[93] [Energy = ½ Capacitance $\times$ (Voltage)^2] or for desalinization.[94] Pt-impregnated carbon aerogels have also been investigated as monolithic fuel-cell electrodes.[95]

What carbon aerogels have not yet offered is new insight into the nature of carbon or the surface character of electrochemical carbons. In contrast, even with the limited number of conductive metal oxide aerogels under study, new phenomena are being observed when the conductive oxides are synthesized as aerogel rather than as xerogel or as micrometer-sized polycrystalline particles. Some of the significant issues and opportunities provided by the oxide-based aerogel systems are described below. It should be appreciated that all of the as-prepared aerogels described below are hydrated transition metal oxides and that thermal processing typically does not remove all of the structural water.

Vanadium oxide aerogels

Since the ability to form aerogels is a property of gels in general,[7,96] it is not surprising that the vanadium oxide system, with its well-established sol–gel chemistry, has received the most attention of the conductive oxides. V_2O_5 gels have been known for over 50 years, but it was the research by Livage and colleagues using sol–gel chemical synthesis that renewed interest in these materials in the 1980s.[97] The resulting xerogels were shown to possess a variety of electrical and optical properties; however, it is their electrochemical properties that provide the basis for the discussion in this review.

Table 1 Physical properties for various electrically conductive transition metal oxides as a function of their preparation as aerogels or ambigels

System	Preparation/drying method[a]	Surface area/$m^2\ g^{-1}$	Average pore diameter/nm	Pore volume/$cm^3\ g^{-1}$
V_2O_5 [35,36]	alk/supercritical CO_2	280	8	0.50
	alk/ambient pentane	185	34	0.48
	alk/acetone (xerogel)	<10	3	<0.01
V_2O_5 [106]	aq/supercritical CO_2	450	20	
	aq/ambient (xerogel)	<5		
V_2O_5 [104]	alk/supercritical CO_2	325		1.2
V_2O_5 [103]	alk/supercritical ethanol	140–200		
$(PPy)_{2.0}V_2O_5$ [119]	alk/supercritical CO_2 (pre-polymerization)	140		
$(PPy)_{1.0}V_2O_5$ [119]	alk/supercritical CO_2 (co-synthesis)	290	16	1.1[b]
	alk/ambient pentane (co-synthesis)	190	17	0.8[b]
MoO_3 [35,124]	alk/supercritical CO_2	180	30	0.6
	alk/ambient pentane	280	7	0.52[c]
	alk/acetone (xerogel)	<10	3	<0.1
RuO_2-TiO_2 [1]	alk/supercritical CO_2	75–85	22[d]	0.44[d]
α-MnO_2 [38] (cryptomelane)	aq/supercritical CO_2	210	16	0.80
	aq/ambient hexane	190	21	1.1
	aq/ambient water (xerogel)	180	5	0.31
MnO_2 [132] (birnessite)	aq/supercritical CO_2	230	21	1.0
	aq/ambient hexane	220	14	0.64
	aq/ambient cyclohexane	220	25	1.2
	aq/ambient water (xerogel)	210	10	0.50

[a]alk: gel synthesized using metal alkoxide precursors; aq: gel derived from an aqueous preparation route. [b]Unpublished data, J. Harreld and B. Dunn, UCLA. [c]Unpublished data, W. Dong and B. Dunn, UCLA. [d]Unpublished data, J.W. Long and D.R. Rolison, Naval Research Laboratory.

The ability of V_2O_5 xerogels to intercalate lithium reversibly has been reported by several groups and it is well established that xerogels exhibit improved capacity for lithium (*i.e.*, moles of Li per mole of V_2O_5) as compared to crystalline (orthorhombic) V_2O_5.[98–101] The lithium capacity of aerogels is even higher than that of xerogels, as detailed below, so electrochemists and materials scientists now have an opportunity to study how surface-to-volume ratios and the morphology of solid and pore (being and nothingness!) on the nanoscale influence electrochemical behavior.

Vanadium oxide aerogels have been prepared by supercritical drying at high temperature (from ethanol)[102,103] and low temperature (from CO_2).[104–106] Ambient-pressure methods have also been reported.[35] The chemical syntheses used to form V_2O_5 aerogels have been varied as well, and include hydrolysis of vanadium alkoxides[102–104] and protonation of vanadates in aqueous solution.[105,106] The resulting materials possess the familiar low density and high surface areas typical of aerogels, although in light of the prior discussion, it is not surprising that lower surface areas are observed after high temperature SCD (see Table 1).

TEM indicates that V_2O_5 aerogels possess the characteristic ribbon morphology of V_2O_5 gels. As shown in Fig. 7, V_2O_5 ambigels also exhibit this morphology, although these materials have a somewhat higher density than SCD-derived aerogels. X-Ray diffraction studies carried out on the aerogels indicate that the high temperature of ethanol SCD (255 °C) leads to some crystallization.[102,103] Materials prepared by either SCD with CO_2 or ambient methods exhibit nanocrystalline characteristics where the 00*l* and *hkl* reflections are consistent with the ribbon morphology.[105–107] Qualitatively, the aerogel materials processed at low temperature exhibit a substantially greater degree of amorphous character than do vanadium oxide xerogels.

An important consideration for electrochemical properties is the pore-size distribution. Fig. 8 compares the pore-volume dependence on pore size for different preparations. Although Scherer questions the interpretation of such information because of the influence of the pore-geometry model used to analyze the resulting data,[108] the data in Fig. 8 suggest that morphologies can be obtained in which the pore volume can be either evenly distributed over a range of pore sizes or confined within a relatively narrow distribution.

The literature covering the electrochemical properties of

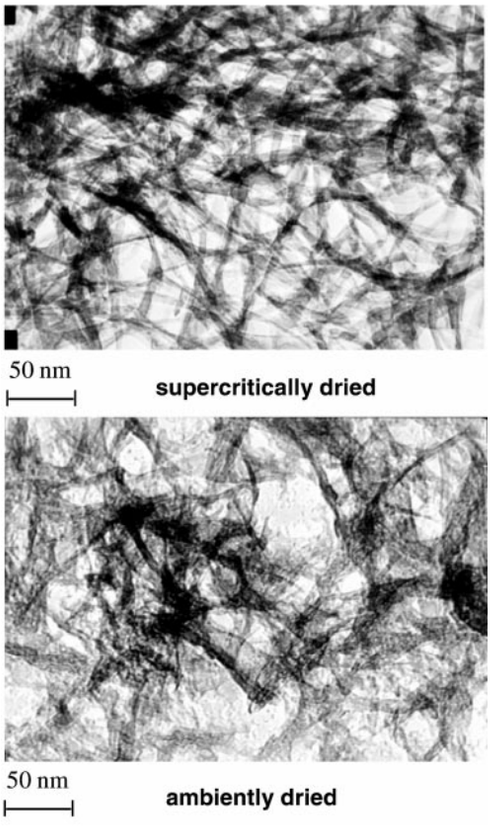

Fig. 7 Transmission electron micrographs comparing vanadium oxide gels dried by (top) supercritical drying from CO_2 to form an aerogel and (bottom) ambient-pressure evaporation of hexane to form an ambigel.

V_2O_5 aerogels is not extensive, but does appear consistent. Several experiments now indicate that the solid-pore architecture of the aerogel contributes to the degree of lithium-ion insertion, leading one to surmise that the aerogel represents a different host material than does a xerogel of the same nominal composition.[105–107,109] The first studies to indicate this behavior were the voltage–composition curves from GITT (galvanostatic-interrupted titration technique[110]) measurements.[105,106] These experiments showed that 4 Li per V_2O_5

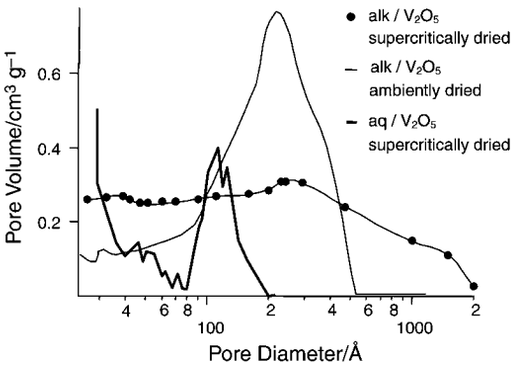

Fig. 8 Dependence of incremental pore volume on pore diameter for V_2O_5 (•) aerogel—alkoxide preparation/supercritical drying from CO_2;[35] (–) aerogel—aqueous preparation/supercritical drying from CO_2;[106] and (–) ambigel—alkoxide preparation/ambient-pressure drying from pentane.[35]

could be cycled reversibly. V_2O_5 xerogels also electrochemically titrate to 4 Li per V_2O_5; however, the equilibrium potential measured for this degree of lithiation is much lower for the xerogel—1.8 V (*vs.* Li) in comparison to 3.0 V for the aerogel. The equilibrium potential behavior is further supported by measurements of the open-circuit potential for chemically lithiated V_2O_5 aerogel. The specific energy calculated from these curves gives values in excess of 1600 W h kg^{-1}, substantially greater than that of the micrometer-sized polycrystalline intercalation electrode materials utilized in lithium secondary batteries,[105] *e.g.*, $LiCoO_2$ or $LiMn_2O_4$.

Recent experiments indicate that further lithiation is possible, with over 5 Li/V_2O_5 obtained by either chemical or electrochemical reaction.[111] Electrochemical studies demonstrate the promising reversible and large lithium-ion capacities of V_2O_5 aerogels and underscore the promise of aerogels for battery applications. Coustier *et al.* investigated the change in specific capacity at various discharge rates and reported only a decrease of ~25%, from 410 to 310 mA h g^{-1},[112] on increasing the rate tenfold from *C*/40 to *C*/4.[113,114] The latter conditions correspond to a current density of 1.3 mA cm^{-2}, on the basis of geometric rather than BET surface area. Of interest for practical fabrication, the electrode structure for these experiments was prepared by physically mixing the wet gel with carbon and then ambiently drying the mixture. The value of 310 mA h g^{-1} readily exceeds the response for electrode materials in commercial secondary lithium batteries; however, the cycling behavior is not as good. The cycling response at the *C*/4 discharge rate exhibits capacity fading so that ~20% of the specific capacity is lost after 80 cycles, but it is likely that the fading does not represent intrinsic behavior. In a limited study involving only 10 cycles, no capacity fading was observed when the cell was discharged at a rate of *C*/8 (37 mA g^{-1}).[115] The capacity for these cells, ~335 mA h g^{-1}, is reasonably consistent with the values obtained by Coustier *et al.*[114]

The mechanism by which lithium is inserted in the aerogel is still not understood—indeed, when the stoichiometry reaches 4, 5, or 6 Li per V_2O_5, it is not clear that insertion (or intercalation) is the correct description of the Li-V_2O_5 associative process. In keeping with such concerns, results from X-ray photoelectron spectroscopy (XPS) and X-ray absorption spectroscopy (XAS) suggest that the oxidation state of the vanadium oxide aerogel is only slightly affected as the numbers of Li per V_2O_5 vary up to nearly 6 lithium.[111] XAS results indicate that V_2O_5 xerogels exhibit a linear shift to V(IV) oxidation state with increasing lithium content up to 2 Li per V_2O_5.[116,117] However, *in-situ* XAS studies of V_2O_5 xerogels undergoing electrochemical lithiation show that the near-edge portion of the vanadium K-edge remains at energies consistent with an oxidation state of V(IV),[118] even for Li/V_2O_5 > 2.[117] An invariant V(IV) near-edge energy indicates

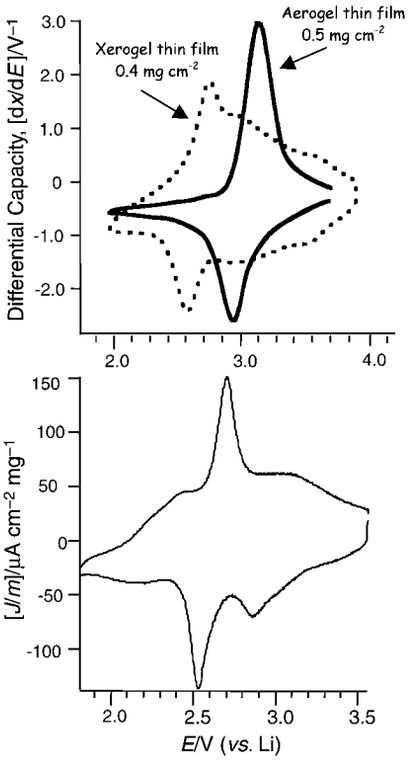

Fig. 9 Cyclic voltammograms in 1 M $LiClO_4$/propylene carbonate electrolyte of vanadium oxide aerogels and xerogels derived from different synthetic routes, which emphasizes the potentials at which lithium-ion insertion occurs. Compare an alkoxide-prepared V_2O_5 aerogel [(bottom; Fig. 6 of ref. 154; scan rate = 0.1 mV s^{-1}). Reprinted from Int. J. Inorg. Mater., **1**, J. H. Harreld, B. Dunn and L. F. Nazar, "Design and synthesis of inorganic–organic hybrid microstructures", 135–146. Copyright [1999], with permission from Elsevier Science.], which has two distinct faradaic redox couples, with one prepared from an aqueous route [(Fig. 6a of ref. 106; scan rate = 0.1 mV s^{-1}). D. B. Le, S. Passerini, J. Guo, J. Ressler, B. B. Owens and W. H. Smyrl, *J. Electrochem. Soc.*, 1996, **143**, 2099—Reproduced by permission of the Electrochemical Society.], which has one faradaic couple.

that additional Li stoichiometry beyond 2.0 cannot arise from a coupled electron/Li^+ insertion into the V_2O_5 lattice. We will discuss further the implications of these results and the apparent electron–Li^+ imbalance of electrically conductive oxide aerogels as battery materials.

In related experiments, cyclic voltammetry has been used to provide some insight concerning the nature of the site(s) of lithium-ion association in electrically conductive aerogels.[119] The results suggest that the specific synthesis route may influence the behavior of lithium-ion association (Fig. 9). V_2O_5 aerogels prepared using alkoxide precursors have two potential sites for lithium insertion at 2.5 V and 3.0 V, while the aqueous system exhibits only one site at 3.0 V. It is interesting that the former material (with two voltammetric reduction peaks) closely resembles that of xerogels prepared by the aqueous method.

Another feature of V_2O_5 aerogels is that the very high ionic capacity extends to ions other than lithium. Substantial capacities for the polyvalent cations, Mg^{2+}, Al^{3+} and Zn^{2+}, were reported for this host material.[120] V_2O_5 xerogels also serve as host structures for polyvalent cations;[97] however, the level of intercalation with the xerogel, 0.33 equiv mol^{-1}, was an order of magnitude less than that with the corresponding aerogel where stoichiometries of 4 Mg^{2+}, 3.33 Al^{3+} and 2.75 Zn^{2+} per V_2O_5 were obtained. Equilibrium potential–composition curves for these systems are comparable to each other and are within a few hundred millivolts of the curve for lithium. This energetic equivalence indicates that the feature controlling the voltages is the host structure (*i.e.*, the V_2O_5 aerogel), with the specific cation being less of a factor. In electrochemical

tests, the polyvalent ions were transported between the working and counter electrodes suggesting that high energy intercalation batteries based on Mg^{2+}, Al^{3+} and Zn^{2+} may be feasible.

Molybdenum oxide aerogels

Another transition metal oxide system that offers useful electrochemical properties is molybdenum oxide. A number of molybdenum oxides undergo reversible lithium intercalation–deintercalation reactions and the orthorhombic form of MoO_3 exhibits substantial lithium capacity (1.5 Li/Mo) with good discharge properties.[121] The presence of mixed electron–proton conducting, mixed-v/vi valent hydrous MoO_3 in Pt–Mo anode electrocatalysts improves the CO tolerance of reformate-fed fuel cells.[122]

Although some prior work on the use of sol–gel methods to prepare molybdenum oxides has been reported, these efforts only led to particulate sols and powders. In order to create a three-dimensional network structure and prepare monolithic gels, a sol–gel method involving ligand complexation of the alkoxide precursor was developed.[123] Complexation suppresses formation of terminal Mo=O bonds enabling Mo–O–Mo bridges to form. Aerogels were prepared by both SCD and ambient methods, with the latter leading to surface areas of nearly 300 $m^2\ g^{-1}$. The significance of this synthetic route is that it is generally applicable to other transition metal oxide systems whose precipitous rates of hydrolysis and condensation prevent them from being conveniently prepared as gels.[12]

At the present time only initial measurements of the electrochemical properties of molybdenum oxide aerogels have been made.[124] Lithium can be cycled reversibly in these aerogels, with the amount dependent upon the structural characteristics of the material. Amorphous aerogels (corresponding to a composition of $MoO_3{\cdot}0.8H_2O$) intercalate 1.1 Li/Mo while a nanocrystalline aerogel (nominally MoO_3) intercalates nearly 1.5 Li/Mo. The latter represents a rather high value for this material.

Manganese oxide aerogels

The various crystalline structures of manganese(iv) oxide are being actively explored as lithium-ion insertion materials as lower cost and lower toxicity replacements for $LiCoO_2$ in lithium-ion batteries. Unlike V_2O_5 or MoO_3, MnO_2 offers a number of polymorphs, ranging from spinel to layered to microporous tunnel structures, which exhibit a spectrum of Li capacities and cycle reversibility (or irreversibility).[125] A key problem with these materials is conversion of the starting MnO_2 polymorph into a spinel structure as Mn(iv) is reduced to Mn(iii) and lithium ions are inserted into the structure. High levels of cell discharge, which generates more and more Mn(iii), create physical changes in the lithiated mixed-valent oxide (due to a Jahn–Teller distortion of the $Mn^{III}O_6$ octahedral core[126]) that effectively removes lithium capacity.[125,127]

Sol–gel-syntheses of xerogel forms of MnO_2 have also expressed various polymorphs,[128,129] and some reports of amorphous MnO_2.[130,131] Recent efforts have focused on using sol–gel syntheses to form ambigels and aerogels of MnO_2 [38,132] and ambigels of Li_xMnO_2.[37] The Li_xMnO_2 ambigel (dried from hexane) was derived from sol–gel reaction of $LiMnO_4$ and lithium fumarate. The as-dried material exhibited a sponge-like morphology and was reported to be amorphous by X-ray diffraction. Annealing (to remove water and residual carbonaceous species) led to broad diffraction peaks that were possibly, but could not be definitively, assigned to Li_2MnO_3 rock salt or spinel Li_2MnO_4. Composite pellets of $Li_{0.9}MnO_{2.5}$ ambigel with carbon and binder were electrochemically cycled at slow rates in Li^+ electrolyte and shown to cycle 1.7 Li/Mn, which is consistent with high capacity, manganese oxyiodide cathodes.[133] Pelletized $Li_{0.9}MnO_{2.5}$ was also able to deliver 150 A h g^{-1} in a high rate discharge.[37b]

$K_\delta MnO_2$ xerogels, ambigels (dried from hexane), and aerogels have also been made using permanganate (K^+) oxidation of an organic reducing agent,[38] following the sol–gel preparation of Livage and co-workers.[134] In this study, Long *et al.* explored the effect on electrochemical lithiation (capacity and rate) of the pore-oxide architecture of sol–gel-derived α-MnO_2 (cryptomelane) in the various forms. Very high surface area materials were derived ($>250\ m^2\ g^{-1}$) for all three dried gels, but the pore size distributions differed, with the aerogel and ambigel forms of cryptomelane having pores sized >8 nm, while the xerogel had a narrow pore distribution centered at 9 ± 3 nm. The Li capacity trend for these materials obtained by rapid voltammetric cycling (2 mV s^{-1}) was: aerogel > ambigel > xerogel > > polycrystalline cryptomelane.[38] Although α-MnO_2 is not a first choice as a Li-ion insertion solid among the MnO_2 polymorphs, this study shows that high rate Li capacity for conductive oxide aerogels exceeds that of the corresponding xerogel and polycrystalline materials. This study also indicates that it is important and possible to control the pore morphology. Control over the pore–solid architecture has also been achieved for high-surface-area gels of birnessite, a layered MnO_2 polymorph with better Li-ion insertion and deinsertion properties than cryptomelane, and the electrochemical properties of these gels are being studied.[132]

Mixed-phase ruthenium oxide–titanium oxide aerogels

Another material that demonstrates the unique electrical and electrochemical properties of aerogels is the mixed-oxide system RuO_2–TiO_2. These compositions, when expressed as fully dense phases, are used as electrocatalysts, including as components in dimensionally stable anodes for the commodity production of chlorine from brine.[135] The ability to form these materials as high surface area aerogels may lead to catalytic electrodes with enhanced reaction rates, because the aerogel's high surface area is readily accessible by reactants (*i.e.*, catalytic substrate) in the liquid electrolyte. RuO_2 is a d-band metallic conductor ($\sigma\sim2\times10^4$ S cm^{-1});[136] however, for electrocatalysis, the more active form is a hydrous defective oxide, RuO_xH_y,[137,138] which retains electronic conductivity ($\sigma\sim1$ S cm^{-1}), but which also is a proton conductor. Hydrous RuO_2 is of interest for energy storage because the pseudocapacitance associated with proton and electron injection leads to specific capacitances of 720 F g^{-1}.[139,140]

The results reported by Swider *et al.* provide important insight into the ability of aerogels to serve as amplifiers of surface-dominated effects.[1,141] The sol–gel synthesis of $(Ru_x$–$Ti_{1-x})O_2$ ($x=0$, 0.14, 0.2, 0.32) involved modifying an alkoxide preparation for TiO_2 with a ruthenium precursor, $RuCl_3$, refluxed in ethanol. Monolithic aerogels, formed by SCD with CO_2, were characterized after annealing treatments at $\sim400\ ^\circ C$ which removed the chloride and alkoxide. The resulting materials consisted of ~10 nm nanocrystallites of primarily phase-separated TiO_2 and RuO_2 (these rutile phases can only form a solid solution of a few mol% RuO_2 in TiO_2 [142]). These mixed oxide aerogels exhibited surface areas of 85 $m^2\ g^{-1}$, comparable (once normalized for mol%) to that of the corresponding pure TiO_2 aerogel.[1,143]

The most significant feature exhibited by the RuO_2–TiO_2 aerogels is that their electrical properties differ markedly from those of the bulk material. By measuring complex impedance under different atmosphere-controlled conditions, Swider *et al.* established that electrical transport in the aerogel is from mixed conduction of electrons and protons, with proton conduction arising from transport in the hydrous layers on the surface of the RuO_2 portion of aerogel network.[1,141] Such hydrous layers are present in bulk materials;[144,145] however, the bulk electronic conductivity dominates transport properties, so

that the hydrous surface, which comprises a small fraction of the total volume, is not independently characterized. In contrast, surface transport processes play a much larger role in aerogels because of their unique morphology in which the material, despite its bulk dimensions, is nominally all surface. With regard to electrochemical behavior, these results suggest that hydration of the ruthenium oxide phase may influence electrocatalysis and even pseudocapacitance to a far greater extent than was previously anticipated.[139,140,146,147]

An aspect that may have significant impact in future work on aerogels is that the authors used traditional defect solid-state chemistry to provide insight into how specific hydration and oxidation reactions influenced aerogel transport properties. Using Kröger–Vink notation to describe the various chemistries in the context of mass, site, and charge balance in the oxide,[148] the authors showed that the following equilibria (eqn. 9–11) explained the electrical properties of the RuO_2–TiO_2 aerogels. In eqn. 9, a perfect rutile RuO_2 lattice is in equilibrium with a defective ruthenium oxide (containing oxygen-ion vacancies [$V_O^{\bullet\bullet}$, charge balanced by Ru^{3+} centers [Ru_{Ru}']) under a partial pressure of oxygen. The highest electronic conductivity is obtained for crystalline, non-defective RuO_2, so flowing oxygen over imperfect $(Ru_{0.32}$–$Ti_{0.68})O_2$ aerogel improves its electronic character.[1,141]

$$2Ru_{Ru}' + 3O_O + V_O^{\bullet\bullet} + {}^1/_2O_{2(g)} \Leftrightarrow 2Ru_{Ru} + 4O_O \quad (9)$$

In eqn. 10, an oxygen vacancy plus an O^{2-} ion in its lattice site [O_O] equilibrate with water in the atmosphere to create protonated O^{2-} on the oxygen-ion site [$OH_O^{\bullet}$]. Thus, the real (*i.e.*, defective) material acts as a proton conductor.[1]

$$2OH_O^{\bullet} \Leftrightarrow O_O + V_O^{\bullet\bullet} + H_2O_{(g)} \quad (10)$$

In the real material, with its proton–electron conductive surface amplified by the high surface-to-volume ratio of the aerogel, the influence of both water and oxygen on electrical transport is given by eqn. 11.

$$2Ru_{Ru}' + 2O_O + 2OH_O^{\bullet} + {}^1/_2O_{2(g)} \Leftrightarrow 2Ru_{Ru} + 4O_O + H_2O_{(g)} \quad (11)$$

These gases act as countering equilibria on the charge transport—an increased partial pressure of oxygen oxidizes Ru^{3+} centers to Ru^{4+}, but dehydrates the surface and lowers the proton portion of the conductivity (Fig. 10), thereby increasing the total impedance of the aerogel. Ionic conductivity is proportional to the number of carriers, so when re-exposed to humidified air, the total impedance of the RuO_2–TiO_2 aerogel decreased.[1]

At temperatures above 100 °C, the electrical response becomes markedly more resistive, until at temperatures above 300 °C (under dry argon), the capacitive component of the impedance disappears and a pure electron response occurs. The pure electron response is less resistive at higher temperatures, which indicates that thermally activated electron transport, either a small polaron or semiconduction mechanism, is operative.[141]

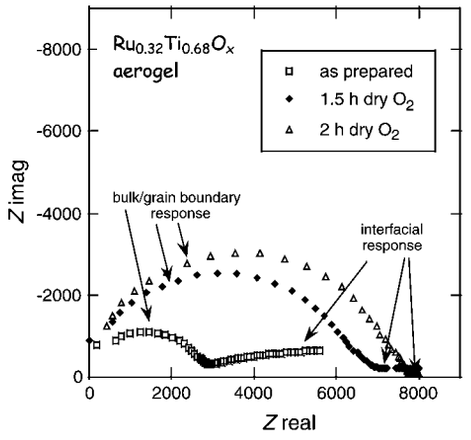

Fig. 10 The impedance of a mixed-phase RuO_2–TiO_2 aerogel depends on the partial pressure of water and oxygen in the bathing atmosphere, which indicates that mixed electron and proton conductivity occurs in this nanoscale mesoporous material.

Examining the RuO_2–TiO_2 aerogels' electrochemical, rather than electrical, properties highlights the difference that exists between surface and bulk, even for nanoscale materials. $(Ru_{0.32}$–$Ti_{0.68})O_2$ aerogels, whose electrical transport is controlled by the mixed electron- and proton-conducting RuO_xH_y surface, exhibited low electrochemical capacitances more typical of crystalline, bulk RuO_2 (contrast 720 F g^{-1} for $RuO_2{\cdot}0.5H_2O$ [139] *vs.* <1 F g^{-1} for anhydrous RuO_2 [140]). In this respect, information on the bulk nature of the nanoscale ruthenia domains in the mixed-oxide aerogel, such as that provided by X-ray diffraction (which confirmed that rutile RuO_2 was formed), was a better predictor of the ability of the aerogel to store charge. Normalizing to the specific capacitance expected for crystalline, anhydrous RuO_2 indicated that essentially all the ruthenia domains in the aerogel were electrochemically addressable.

The conjunction of the electrochemical and electrical behavior of RuO_2–TiO_2 aerogels underscores the difficulty in characterizing and predicting the properties of conductive oxide aerogels. For the RuO_2–TiO_2 aerogels, X-ray diffraction could predict the low level of electron–proton storage, but it mispredicted the electrical transport properties. Such structure–function mishaps are to be expected as the electrically conductive oxides are diversified compositionally and used as electron-ion reactive materials.

Organic/inorganic hybrid aerogels

The synthesis of organic/inorganic hybrid materials has received considerable attention in the past several years because of the prospect of developing materials with unique microstructures and properties.[84,85] The combination of conducting polymers with transition metal oxides is of substantial interest and the synthesis of these 'nanocomposites' by a variety of methods including sol–gel approaches has been reported.[149] The general objective in synthesizing these hybrid materials is to incorporate the conducting polymer within the lamellar spaces of layered inorganic oxides. Since the layered V_2O_5 materials are readily prepared by sol–gel approaches, xerogels utilizing V_2O_5 as the inorganic host have been investigated and recent studies have described the electrochemical properties of polyaniline/V_2O_5 and polypyrrole/V_2O_5 xerogels,[150] and a self-doped sulfonated, alkylated polyaniline/V_2O_5 xerogel.[151] Lithium insertion in these hybrid materials was reversible and enhanced Li^+ diffusion rates in the electrode were observed.

Hybrid aerogels of conducting polymer–V_2O_5 have also been synthesized; however, the approach is quite different from that of the xerogel work. With the aerogel materials, the objective is to attain two interpenetrating networks: V_2O_5 to achieve lithium intercalation and the conducting polymer to provide an electronically conducting network.[119,152] This approach would circumvent the need to add carbon to electrode structures because of the low electronic conductivity of the transition metal oxide. A key feature in designing this hybrid material is the need to have a homogeneous distribution of the conducting polymer so that good access to the vanadium oxide phase is achieved.

Nanocomposite aerogels composed of polypyrrole (PPy) and V_2O_5 have been synthesized by two different sol–gel-based methods. One approach is a cosynthesis route where the organic and inorganic networks are polymerized simultaneously from a common solvent.[152–154] The second approach involves sequential polymerization of each component; V_2O_5

gels are impregnated with the pyrrole monomer, which then oxidatively polymerizes as initiated by V(v) centers.[154] Hybrid aerogels are then formed by either low temperature SCD or ambient-drying methods.

The electrochemical properties of the hybrid aerogels critically depend on controlling the microstructure of the hybrid. The post-gelation synthesis method leads to relatively poor electrochemical properties because the inhomogeneous distribution of PPy limits access to the V_2O_5 phase. In comparison, cosynthesis offers excellent microstructural control and a homogeneous distribution of the PPy phase is achieved. Reversible lithium capacity in excess of 3 Li/V_2O_5 is obtained, although the hybrid does not exhibit improved macroscopic conductivity. The limitation in developing higher conductivity is the inability to oxidize PPy into its high conductivity state. The addition of an oxidizing agent at the necessary concentrations inhibits V_2O_5 gelation. A factor that can limit lithium capacity is that of V^{4+} centers created from the polymerization of the monomer. This capacity, however, can be regained by oxidation treatment and the resulting PPy/V_2O_5 aerogel hybrid materials exhibit increased lithium capacity as compared to the V_2O_5 aerogel.[119]

Recent results with a second organic/inorganic aerogel system show that the addition of the conducting polymer can indeed lead to enhanced conductivity. In this work, PPy/MoO_3 hybrid materials were synthesized by a co-solvent method and the electrical conductivity of the resulting material, 4×10^{-3} S cm^{-1} at room temperature (Fig. 11), was approximately 100 × larger than that of the pristine MoO_3 gels.[155] This value is also ten times greater than that of a system in which the conducting polymer (polyaniline) was intercalated into the crystalline MoO_3 structure.[156] PPy was adventitiously doped by incorporating Cl^- derived from the isopropoxide precursor, $MoCl_3(O^iPr)_2$. The doping of PPy by Cl^- has been reported previously and shown to stabilize the PPy structure.[157]

Electrically conductive composite aerogels

A conductive gel network is not the only way to make an aerogel electrically conductive. In recent work Morris *et al.* showed that silica sol could be used as a "nanoglue" to fabricate guest–silica composite gels and aerogels.[158] The guest solid can be essentially any size (spanning six orders of magnitude from nanometers to millimeters) or any chemical nature (metal, metal oxide, carbon, ceramic, semiconductor, polymer). Fig. 12 shows a transmission electron micrograph of a colloidal gold–silica composite aerogel in which the silica colloids and metal colloids are readily differentiated.

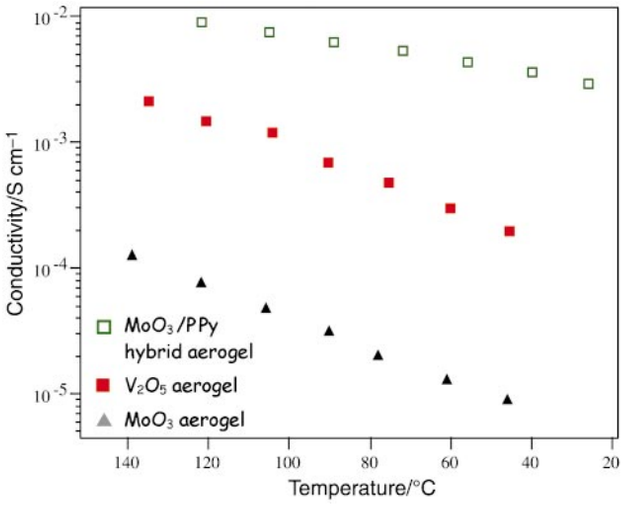

Fig. 11 Electrical conductivity of V_2O_5 and MoO_3 aerogels and polypyrrole–MoO_3 hybrid aerogel.

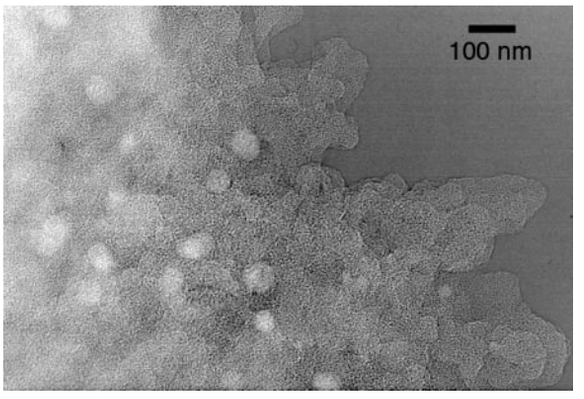

Fig. 12 Transmission electron micrograph of a colloidal Au–silica composite aerogel showing Au colloids (brighter circles) dispersed throughout the amorphous silica aerogel [(ref. 158) Reprinted with permission from C. A. Morris, M. L. Anderson, R. M. Stroud, C. I. Merzbacher and D. R. Rolison, *Science*, 1999, **284**, 622–624. Copyright [1999] American Association for the Advancement of Science.].

Two conditions must be met to establish charge transport paths through the composite aerogel: *(i)* introduce a sufficient volume fraction of the electrically conductive guest (either one that meets a statistical percolation threshold[159] for the dimensionality of the gel,[160,161] or one that can be lower if the guest particles self-associate in the silica sol); and *(ii)* limit the exposure of the guest to the silica sol (by controlling time of exposure or thoroughness of mixing). Vulcan carbon, which is a highly disordered graphitic-like carbon black commonly used in fuel cells and batteries, was chosen as the electrically conductive guest to identify the processing and gelation conditions that would (or would not) yield electron paths through the resulting C–SiO_2 composite aerogel.

The authors report that the morphology of the silica sol controls the ability to achieve electron transport in the C–SiO_2 composite aerogel.[5,158] Through-aerogel conduction was obtained with >6.4 vol.% carbon for the roughly spherical sol characteristic of base-catalyzed silica,[11] while 30 vol.% carbon was insufficient to achieve conductive composite gels using the polymeric sols typical of acid-catalyzed silica as the nanoglue.[158] Turbulent mixing or long contact times yielded non-conductive C–SiO_2 composite aerogels, even when using base-catalyzed silica sol and >6.4 vol.% of carbon.[158] These parametric influences were recently reaffirmed for Bi_2Te_3–SiO_2 composite aerogels, in which micrometer-sized Bi_2Te_3 powder (pretreated to remove insulating surface oxides) produced either insulating composite aerogels after turbulent mixing or end-to-end electronically conductive composite aerogels by minimal exposure of base-catalyzed silica sol to the pretreated Bi_2Te_3 powder.[162]

Another promising application of the nanoglue approach is to create TiO_2–SiO_2 composite aerogel monoliths or crack-free films as an eventual means to create durable photoelectrodes. TiO_2 aerogel, which is typically a mechanically fragile solid when expressed as an aerogel,[16b] can be preformed and pre-annealed to form the desired crystalline state and doping level of TiO_2 and then prepared as a composite aerogel with sufficient connectivity established between the particles of TiO_2 aerogel to ensure through-structure electron paths.[163] Although TiO_2 is an important photocatalyst,[164] and has shown effective photocatalytic activity in aerogel form,[143] it is also of interest as a photoelectrochemical material in nanoscale form, including as a photosensitized electrode in photovoltaic devices.[165] Walker *et al.* have reported that TiO_2 aerogel was more effective for photoelectrochemical oxidation of phenol than were anodic films or sol–gel-derived xerogel films of anatase TiO_2.[166]

Another way to introduce electronic paths into an aerogel

architecture is to use the durable silica network as the support for conductive nanoscale deposits. Ryan *et al.* have developed a sub-0 °C decomposition of RuO_4 to form a massively parallel web of nanowires of crystalline RuO_2 on partially densified silica aerogels.[51] Efforts to deposit RuO_2 by decomposition of such Ru precursors as ruthenocene, ruthenium(III)tris-acetylacetonate, or Ru_3CO_{12} at temperatures greater than 100 °C led to aerogel-supported RuO_2 deposits that were not interconnected electronically.[82,83] The lack of connectivity arose because at the reaction temperatures necessary to decompose the organometallic Ru-based precursors, most of the precursor had volatilized out of the aerogel structure before decomposition could occur and the RuO_2 that did deposit, coarsened, thereby separating neighboring particles.

Unlike the mixed conductivity observed for RuO_2–TiO_2 aerogels,[1,141] silica aerogel modified with an interconnected web of nanoscale crystallites of RuO_2 ($\sim 4\,nm \times 30\,nm$) behaves as a pure electron conductor. Although the silica-supported conductor is nanoscopic, because it is a chemically stable, metallically conductive oxide, it retains its electronic properties upon exposure to oxygen and water. The deposited RuO_2 nanoparticles affect neither the surface area nor the pore volume of the partially densified silica aerogel, which permits these electronically wired silica aerogels to be explored as durable, high surface area mesoporous electrodes.[51] Anhydrous RuO_2 is used in thick-film resistors[167] and as thin-film barrier layers or bottom electrodes in DRAM devices,[168] so this nanowired aerogel may also offer new possibilities to design three-dimensional, nanoscopic electronic circuits.

The electrochemistry of high surface area materials

Inherent physics

The physical nature of aerogels—nanoscale, high surface area solid and a networked, mesoporous volume—imparts physical consequences to their use. Just as the continuous mesoporous network of an aerogel or ambigel serves as a superhighway for molecular reactants or analytes, so it should for the solvent and ions that accompany (and are necessary for) any change in surface charge at an electrified interface. Electron- and charge-transfer reactions at an electrified interface or within an electrode material are hindered unless ions and solvent (and usually solvated ions) can freely approach the electrified interface.

Experimental evidence indicates that the walls of micropores (*i.e.*, the surfaces of pores $<2\,nm$ in diameter) do not contribute usable electrode surface area in well-studied practical electrodes such as porous RuO_2.[138] Studies with microporous carbon electrodes showed that ion mobility into pores $<1\,nm$ was several orders of magnitude less than in open solution.[169] In an aerogel, the usable electrified interface is the outer surface of the solid network, *i.e.*, the walls of the mesoporous network. Ions, reactants, and solvent molecules, as necessary, must approach the enormous nanoscopic electrode interface through the mesoporous network.

Aerogel electrodes are thus a class of through-porous electrodes, but ones in which the pores are not macroscopic. Porous (or three-dimensional) electrodes are well-studied objects, both empirically[170] and by modeling,[171] because they are a design choice for large scale, relatively high surface area electrodes in industrial electroreactors and because practical insertion electrodes in batteries contain macropores. The 2 to 50 nm mesopore range that exists in an aerogel electrode is far finer, though, than that customary in standard porous electrodes. This pore regime, although still large on a molecular or ionic scale, again has physical implications.

Mass transport can be convective or diffusive (and for charged solutes, electromigrational).[172] Forced flow (or transport) of material can be turbulent or laminar. Forced gas flow into aerogels is hindered by the tortuosity imposed by the mesoporous network of an aerogel.[173] Fluidized gas-phase reactors, which are a standard convective reactor design for heterogeneous chemistry, function at high velocities with aerogel particles because the particles reorganize into agglomerates that fluidize smoothly and uniformly, but which have low permeability.[174] Recent work indicates that hydrostatic flow into silica aerogels is feasible and that the plug resistance of the monolith or membrane is lowered markedly by vapor-phase pre-equilibration of the silica surfaces of the aerogel with water.[175] Liquid-phase reactions within aerogels, including electrochemical reactions under flow, are therefore feasible.

Diffusion of an electron-transfer reactant (redox solute) to an electrified interface follows four profiles: *(1)* semi-infinite (or planar) in which the bulk concentration of the reacting species is essentially unaffected by the electroreaction at the electrode surface, but a linear concentration gradient is established between bulk and the electrified interface; *(2)* spherical in which the perimeter-to-surface ratio of the electrode is large such that the initial linear flux of redox solute rapidly converts to non-linear, drawing molecules from a larger volume of solution and effectively achieving a steady-state flux of molecules to the electrified interface; *(3)* finite diffusion in which the volume of the electrochemical cell is so small that bulk electrolysis of all redox solutes occurs in seconds or minutes rather than hours; and *(4)* surface-confined, in which the reactant is tethered directly to the electrode surface and does not diffuse.

All four of these diffusion profiles have been mathematically explored and experimentally verified at smooth electrodes.[176] The expected voltammetric responses (*i.e.*, the current that flows as a function of the potential applied to the electrified interface) for three of these diffusive profiles are shown in Fig. 13. Electrified interfaces with convoluted morphologies that are fractal and have a dimension between two and three, demonstrate a fractal-dimension-controlled electrochemical response to the diffusion of redox solutes to the electrified fractal interface.[177] Fractal electrode structures can be obtained by electrodeposition, electromachining, or corrosion,[178] or by lithographic fabrication of electrode surfaces with patterns of a pre-determined fractal dimension.[179] Chronoamperometry, in

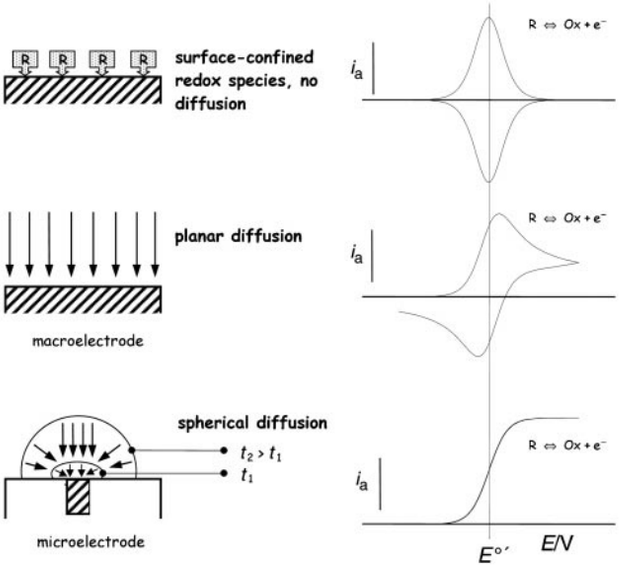

Fig. 13 Voltammetric current–potential plots for three different diffusion profiles in which an electroactive species (redox solute) with a formal potential of $E^{\circ\prime}$ undergoes a reversible one-electron oxidation under conditions of surface confinement (no diffusion), semi-infinite (planar) diffusion, or steady-state (spherical) diffusion at time t_2 (at time t_1, diffusion is converting from planar to spherical); i_a represents anodic current.

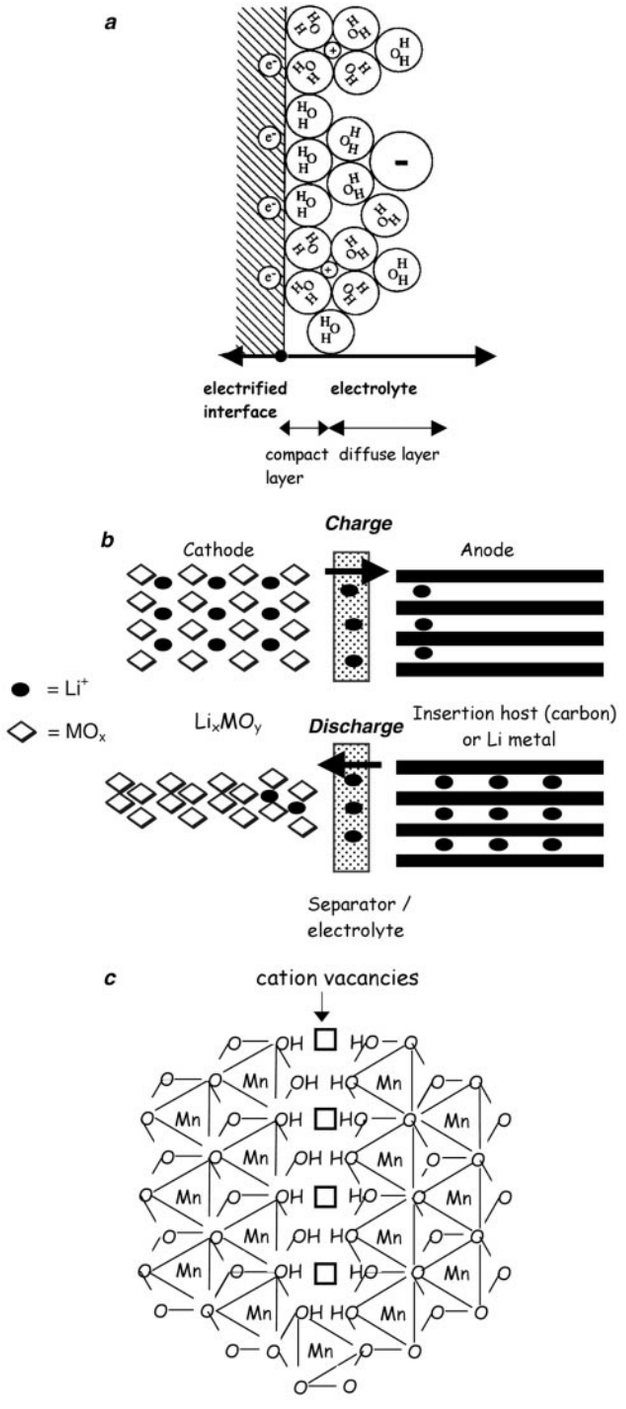

Fig. 14 The three types of charge uptake at an electrified cation-insertion material; (*a*) formation of a capacitive charge (double layer) at an electrified interface poised at (in this instance) a potential negative of its point of zero charge; (*b*) electrochemical intercalation of Li^+ into the cathode of a battery [(after ref. 127) Reprinted with permission from M. Winter, J. O. Besenhard, M.E. Spahr and P. Novák, *Adv. Mater.*, 1998, **10**, 725–763. Copyright [1998] Wiley-VCH.]; (*c*) proposed cation vacancies, and accommodation of vacancy-balancing protons in MnO_2 [(after ref. 196) P. Ruestchi and R. Giovanoli, *J. Electrochem. Soc.*, 1998, **135**, 2663–2669—Reproduced by permission of the Electrochemical Society.].

which the time-dependent current is monitored after a potential step from a potential of no electroreaction to one where faradaic electron transfer occurs, is normally used to determine if diffusion is under fractal-dimensional control in these types of electrode interfaces.[177–179]

Xerogels and aerogels have fractal-like character as determined by scattering experiments,[161,180] so it is conceivable that diffusive mass transport of solutes to an electrified gel interface may be controlled by the fractal dimension of the solid. When the electrode itself is undergoing electroreaction, as occurs during lithium-ion insertion, mass-transport issues may become more intricate. The diffusion of Li^+ to the electrified gel network through the electrolyte solution that fills the mesoporous network may exhibit fractal-dimensional control, while the nanoscale transition-metal-oxide colloids that comprise the electrode may act as extremely thin-layer electrochemical cells for Li-ion charge and discharge, and therefore be governed by finite-diffusion control. In the first studies to explore this behavior, the voltammetric response of α-$K_\delta MnO_2$ ambigels and aerogels undergoing Li-ion insertion and deinsertion exhibited finite-diffusion characteristics.[38b] The electrochemical response of these high-surface-area, high porosity gels may, for certain electrochemical reactions, offer a time signature for mass transport that is a blend of finite-diffusion control in the solid network and fractal-dimensional control of diffusion of necessary electroreactants through the pore network.

Diffusive mass transport into an aerogel interior occurs at rates consistent with diffusion in gases (for gas-phase solutes) or liquids (for liquid-phase solutes). Leventis, Rolison, and co-workers have used the aerogel morphology to demonstrate extremely rapid sensing of gas-phase O_2 by fluorescence quenching.[181] The authors estimated that the steady-state fluorescence response of diazapyrenium-modified silica aerogel monoliths tracked the ingress of analyte near the speed of open-medium diffusion.[182,183] The rates of mass transport visibly evident in the fluorophore-modified aerogel, and especially the ability of RuO_2–TiO_2 aerogels to store electron–proton charge commensurate with the mass of ruthenia domains present in the material,[140] demonstrate the feasibility of solvent-ion diffusive transport into the entire aerogel interior on electrochemically reasonable time scales.

But how fast can an electrically conductive oxide aerogel respond electrochemically? Not only must ions and solvent move at rates near those typical of the bulk medium, but also the ability of the electrical circuit to charge the surface of the aerogel must be considered. Two inescapable facts of physics are *(i)* the measure of how fast an electrical circuit responds is dictated by its *RC* time constant and *(ii)* capacitance (*C*) at an electrode surface (which is due to a layering of mobile ions of opposite sign to the charge on the electrified surface: *i.e.*, double-layer or Helmholtz capacitance) is directly proportional to its area, see Fig. 14a. The larger the area of electrode surface, the more sluggish is the response of the electrical system to a change in potential. Large-surface-area electrodes in electrochemistry can approach 0.01 to 0.1 m^2. Electrically conductive aerogels have areas $>100\ m^2\ g^{-1}$, which means that aerogels unavoidably have large *RC* time constants. As a consequence of the physics of an electrical circuit with a large *RC* time constant, aerogel electrodes cannot change surface charge (and therefore assume an imposed potential) at the rates expected for electrodes of customary surface area.

These unavoidable facts of physics have real implications for battery electrodes containing aerogels as the active material. Even when the slow solid-state diffusion step is minimized in ion-insertion reactions due to the nanoscale nature of the oxide, the enormous surface area of the aerogel material adds a slow step into the charge/discharge processes due to the innate *RC* time constant of the aerogel electrode.

What does it mean to intercalate Li^+ in an aerogel?

The starting point to understand the nature of ion uptake in electrically conductive aerogels is to first review the differences between batteries and capacitors. These distinctions have been well discussed by Conway.[184] It is necessary to distinguish between "double-layer capacitors", "supercapacitors" (which are double-layer capacitors where the electrodes have enor-

mous surface areas approaching 1000 $m^2\ g^{-1}$), and ultra- or "pseudocapacitors". The last are based on faradaic electron insertion with accompanying cation insertion (hence the term: pseudocapacitance) and are much more relevant for the aerogel materials.

Batteries normally involve well-defined 3-D phases and, as such, have unique chemical potentials. Ideally, the chemical reactions occur at a single potential until one phase is converted to another. In contrast, when the battery system involves a range of oxidation states, a unique potential does not usually occur. Supercapacitor processes are fundamentally different from those in batteries in that electron insertion is not involved, but 2-D surface reactions are. Pseudocapacitance involves a continuous range of potentials and redox processes that require successive electron transfer. The latter is well established in the hydrous RuO_2 system where there is a double-injection process as both protons and electrons are inserted into the oxide. Double-layer capacitance can be readily distinguished from that of pseudocapacitance on the basis of the magnitude of the specific capacitance ($F\ cm^{-2}$); the specific capacitance for pseudocapacitance is 10 to 100 times larger than that observed at carbon/H_2O interfaces (*ca.* 10–30 $\mu F\ cm^{-2}$).

The intercalation of lithium into intercalation hosts has been described as a quasi-2-D process (Fig. 14b).[127,185] During discharge there is a continuous decrease in potential, provided that phase changes do not occur. Moreover, the amount of lithium intercalation depends directly on the amount of faradaic charge passed. Thus, the relation between the potential and the amount of intercalation can be differentiated enabling one to formally associate a pseudocapacitance for intercalation processes. In this way, there is an intrinsic similarity between intercalation-based batteries and pseudocapacitors.

The initial studies of the electrochemical properties of electrically conductive oxide aerogels suggest that these materials possess both battery-like and capacitor-like behavior. The electrochemical studies definitively show that V_2O_5 aerogels provide enhanced capacity for lithium and polyvalent cations as compared to the corresponding xerogel (which in turn provides enhanced capacity relative to fully dense V_2O_5).[186] One reason for this behavior is the far greater accessibility that the aerogel microstructure offers to molecular and ionic reactants through the mesoporous network.

An important factor associated with the porous nature of the material is the dimension of the solid phase that represents the "pore wall". This dimension is rather thin, typically 10 to 50 nm, so that the diffusion distances to be traversed by Li^+ (or other ions) are quite small. In fact, researchers contend that such short diffusion paths lead to rapid injection and release of the intercalated ions, so that diffusion within the solid phase is the limiting factor.[105,106]

The results indicating the battery-like behavior of V_2O_5 aerogels have been described in several publications.[105,106,111,114] Standard battery electrodes were prepared in which the aerogel powders were mixed with a carbon additive and a binder, and the usual charge–discharge experiments were performed. The first evidence of capacitor-like behavior was shown in a coulometric titration experiment where the voltage–time (V–t) response indicated that the V_2O_5 aerogels exhibited capacitor-like behavior at short times ($V \propto t$) with a transition to a diffusion-limited process ($V \propto t^{1/2}$) at longer time.[114b] This result suggests that the aerogel material acts as a capacitor for a thin layer of material (tens of nanometers) closest to the current collector. Beyond that distance, the kinetics becomes diffusion-limited.

Aerogel-based battery electrodes are not expected to exhibit capacitor-like behavior. In fabricating the composite electrode structure, the aerogel particles are likely to be aggregated (Fig. 6a) to sizes in the micrometer range, so that only a diffusion-limited response will be observed. Nonetheless, the coulometric titration does suggest that a proper electrode structure, one that effectively "wires" the aerogel to the current collector, can be expected to exhibit capacitor-like behavior. The "sticky carbon" electrode described by Long and Rolison[140,187,188] seems to provide such wiring (Fig. 6b). By mixing acetylene black (a high purity carbon black) or graphite with a wax, it is possible to prepare a conductive electrode that effectively holds the finely dispersed, high surface area particles at the carbon–wax surface and exposes them to the electrolyte. In a recent study employing the sticky-carbon electrode for V_2O_5 aerogels and ambigels, a strong capacitive response was observed in combination with high Li-to-V_2O_5 stoichiometries.[36]

Related to the battery–capacitor response of aerogel electrodes is the issue of how the enormous surface area contributes to the enhanced capacity for lithium that these materials exhibit. The traditional explanation involves intercalation, where a mobile guest species inserts into a network of empty lattice sites of appropriate size within a rigid host lattice.[189,190] The transition metal ion that is part of the host structure is reduced. The host materials most covalent in nature, such as graphite and conjugated polymers, are able to intercalate both anions and cations. The oxides and chalcogenides of transition metals are more ionic in character. Owing to coulombic interactions in these materials, only cations and electron donors (Lewis bases) can be intercalated. One generally associates intercalation with crystalline structures such as three-dimensional framework structures with empty lattice sites forming channels or cavities, or two-dimensional layer structures where intercalation takes place in van der Waals gaps. Insertion of ions into amorphous structures has received relatively little attention, but it is expected that these structures will have a large number of sites that adapt readily to the size of the inserted species. Recent X-ray absorption studies with amorphous Mn oxyiodide electrodes confirm this expectation as less dramatic structural changes resulted for the amorphous Mn-based oxide relative to crystalline λ-MnO_2, $LiMn_2O_4$, and $Li_2Mn_2O_4$ as the various materials were electrochemically discharged from Mn^{4+} to Mn^{3+}.[191]

In order to intercalate 4 Li/V_2O_5, as intercalation is normally considered in the ionic oxides, the accompanying electron transfer reactions require the formation of V^{3+}. The XPS and XAS results reported recently[111,116,117] indicate not only that such species do not form, but that in fact, very little change in the oxidation state of the vanadium is even observed. Another inconsistent result with the V_2O_5 aerogels involves the capacity of this form of V_2O_5 for polyvalent cations.[120] Ion-exchange experiments with V_2O_5 *xerogels* showed that the number of intercalated ions depended upon valence such that 0.33 equiv mol^{-1} were obtained consistently for various +1, +2, and +3 species.[192] In contrast, the insertion levels for Mg^{2+}, Al^{3+} and Zn^{2+} were approximately ten times greater, ranging from 2.75 to 4 equiv mol^{-1}.

Charge storage in aerogels

The fascinating question to consider regarding the high capacity observed for lithium and the multivalent cations in V_2O_5 aerogels is the nature of charge storage in these nanoscale mesoporous materials and whether the high surface area contributes to this effect. For traditional (low surface area) battery electrodes, the charge held by the double-layer capacitance is a fraction of the faradaic charge capacity of the electrode, which, in the case of lithium batteries, arises from intercalation reactions. Since the published work on the X-ray-determined oxidation state of vanadium in V_2O_5 aerogels indicates that vanadium reduces to V(IV) and no further, there must be another mechanism which enables V_2O_5 to reversibly take-up substantially more than the 2 Li/V_2O_5 associated with the vanadium reduction process.

The research on the RuO_2–TiO_2 system has demonstrated that the aerogel morphology serves to amplify not just the physical amount of the surface, but its surface character as well.[1,141] These results and the wealth of research on aerogel catalysts provide a strong indication that surface amplification is expected to be a fundamental characteristic of all aerogels. Thus, a pertinent question that emerges is what surface chemistry can one expect for V_2O_5? Although the surface chemistry of V_2O_5 is of interest because of the importance of V_2O_5 as an oxidation catalyst,[193] unfortunately, the surface chemistry of nanoscale, mesoporous V_2O_5, characteristic of aerogels, has not been explored. The analysis published by Ruetschi on the nature of the MnO_2 system provides some insight, however.[194–196] In this work, Ruetschi explored a cation-vacancy model (Fig. 14c) and could explain a number of mystifying electrochemical properties for MnO_2,[194] including a thermodynamically driven increase in the cell voltage as the manganese oxide becomes more defective,[195] and the association of protons with cation vacancies and Mn^{3+} centers.[196] It should be appreciated that metal oxide surfaces are inherently defective in that they present a truncated structure with missing atoms. Because aerogels amplify the surface character of transition metal oxides, defects, including those based on cation vacancies, are expected to contribute strongly to the electrochemical properties of these types of materials.

If the cation vacancy hypothesis is extended to vanadium oxide, then mechanisms for the observed electrochemical behavior can be postulated. Vanadium vacancies are likely to be highly charged, arising from the 5+ and 4+ valence of the metal, and negative, because of the inherent properties of cation vacancies. An aerogel with a high concentration of such vacancies must compensate this charge imbalance. In keeping with Ruetschi's model in which protons associate with both cation vacancies in the MnO_2 lattice and electron-generated Mn^{3+} centers,[196] the accessibility of Li^+ to cation vacancies in V_2O_5 would produce an ion current but no accompanying electron transfer to vanadium cations and therefore no generation of V(IV) or lower oxidation states. In this way, the presence of vanadium vacancies can lead to a charging, but non-faradaic process based on the ingress and egress of lithium ions from the aerogel. Non-faradaic processes that give rise to apparently faradaic electrochemical current–voltage–time responses are known and include transfer of non-redox-active ions across liquid–liquid interfaces[197] and protonation/deprotonation at carboxylic-acid-terminated alkanethiol-modified electrodes.[198]

The above mechanisms would explain why lithium uptake goes beyond what one expects for 2 e^-/2 Li^+ per V_2O_5 to electrogenerate V(IV) centers in $Li_2V_2O_5$, as well as explain the high capacity obtained with divalent and trivalent ions. Other defect mechanisms without electron transfer are also possible as oxide systems commonly exhibit defect pairs (*i.e.*, Schottky defects). The work with RuO_2–TiO_2 aerogels also gives evidence that anion vacancies in these solids are present and are intimately involved in the proton-conduction process,[1,141] eqn. 10.

The key issue, however, is the innate ability of aerogels to amplify the surface so that electrochemical properties are strongly influenced, if not dominated, by the presence of defects. The fact that this contribution is observed for aerogels and not V_2O_5 xerogels is attributed to the far lower surface area of the latter. Definitive experiments on the presence of defects in aerogels and xerogels—and the role these defects play in the high cation capacitances of electrically conductive metal oxide aerogels—are in progress.[199]

Re-thinking electrode structures

Why should composites of being and nothingness be used in electrochemical devices exactly as standard bulk forms have always been? As discussed above, the bulk oxides used as battery materials are formulated into a practical electrode by physically mixing the active material (in powdered form) with other structural (*e.g.*, polymer binders) or electrical (*e.g.*, conductive carbon blacks) components. The composite is then pressed or cast onto planar current collectors to create micrometers-thick, layered composite electrode structures. But when the active material has been deliberately created in a nanoscopic form within a continuous mesoporous volume, should the traditional masonry approach to electrode structure be retained?—especially when some fraction of the active material or electrocatalyst within the composite is inevitably occluded, becoming thereby less electron/reactant/fuel accessible?

Conformable electrochemical power sources have been a design goal for decades, thus, accounting for much of the interest in all-polymer batteries[200] based on conducting polymer electrodes and ion-conducting polymer electrolytes.[201] As microelectromechanical devices and sensors scaled into mesoscopic ranges become more standard, electrochemical power sources that are integral to the device environment become a design requirement, rather than a goal. Aerogels are prepared by liquid-phase synthesis, which means that gel and dried gel structures can be conformed to the shape and size demands of an application. As described above, the three-dimensional structure of aerogels with a solid network of active material enveloped by a continuous mesoporous network provides a multifunctional platform—one that integrates being and nothingness to facilitate ready access to electroactive surfaces without occlusion of the active material or electrocatalyst within a microparticulate composite structure.

Challenges and opportunities

This review has explored the prospect that aerogels offer a new direction in electrochemical materials. Although relatively few conductive oxide aerogel systems have been investigated, these materials have, nonetheless, already demonstrated unexpected and exciting electrochemical properties. The chemical and structural considerations with these materials are rather different from those of the thermally insulating oxide aerogels or even the aerogel catalysts. A sufficient number of electrically conductive transition metal oxides have now been synthesized and characterized in aerogel form that certain commonalities in their electrochemical character are apparent. Aerogels unavoidably amplify the surface character of electrically conductive transition metal oxides, which has translated into new properties for cation-insertion battery materials based on aerogels and an improved understanding of mixed-valent, mixed electron–proton conducting oxides of interest in ultracapacitors and fuel cells.

A recurring theme in this paper has been that aerogels represent nanoscale solids whose local chemistry, structural disorder and surface defects have the ability to dominate electrochemical properties. Because our experimental bias lies toward synthesizing and characterizing ordered materials,[202,203] the physical and chemical nature of this new generation of electrochemical materials are poorly understood, especially when they are present only at a surface or exhibit short range order that extends, at most, to a dimension of 1 nanometer. The challenge with these materials is not only to characterize their physical and chemical properties, but also to maintain the desired local chemistry and structure in the face of thermodynamic forces inherent to the application, whether it be the operating temperatures of a fuel cell or electronvolts (eV) of stored (and cycled) energy in a battery.

The following areas will need to make advances singly and in concert to improve our understanding of conductive oxide aerogel systems and to optimize their use: computational and combinatorial exploration with respect to how disordered chemical composition and physical structure may be stabilized

(or pinned); soft, low temperature chemical approaches (*chimie douce*) that synthesize disorder to match (or prod) theory and modeling; and greater imagination in how our experimental tools are used to characterize partial disorder in the solid state. Conductive oxide aerogels have the opportunity to revolutionize the electrode structures and configurations utilized for a wide range of technologically important power generation systems.

Acknowledgements

It is a pleasure to acknowledge our research associates and colleagues who during their sojourns at UCLA and the Naval Research Laboratory have contributed far more than we to the creation and understanding of electrically conductive oxide aerogels: Michele Anderson, Robert Bernstein, Veronica Cepak, Wei Cheng, Winny Dong, John Fontanella, John Harreld, Michelle Korwin, Nicholas Leventis, Jeffrey Long, Erik Lukas, Celia Merzbacher, John Miller, Cathy Morris, Linda Nazar, Jeremy Pietron, Joseph Ryan, Jeffrey Sakamoto, Kurt Salloux, Rhonda Stroud, Karen Swider-Lyons, and Henry Wong. We would especially like to acknowledge our research sponsors (the Office of Naval Research and the Defense Advanced Research Projects Agency) for their support of these studies and, in particular, Karen Swider-Lyons for her insights into solid-state defect chemistry.

References

1 K. E. Swider, P. L. Hagans, C. I. Merzbacher and D. R. Rolison, *Chem. Mater.*, 1997, **9**, 1248.
2 D. R. Rolison and C. I. Merzbacher, in *1999 NRL Review*, Naval Research Laboratory, Washington, DC, 1999, pp. 121–122.
3 J.-P. Sartre, *L'Être et le Néant*, Gallimard, Paris, 1943.
4 J. Fricke, *Sci. Am.*, 1988, **258**, 92.
5 M. L. Anderson, R. M. Stroud, C. A. Morris, C. I. Merzbacher and D. R. Rolison, *Adv. Eng. Mater.*, 2000, **2**, 481.
6 The main applications of aerogel research over the past 15 years can be tracked by the contents of the five Proceedings of the International Symposia on Aerogels: J. Fricke, ed., *Proceedings of the International Symposia on Aerogels*, Springer-Verlag, Berlin, 1986, pp. 1–203; R. Vacher, J. Phalippou, J. Pelou and T. Woignier, eds., *Rev. Phys. Appl.*, 1989, **24**, C4-1; J. Fricke, ed., *J. Non-Cryst. Solids*, 1992, **145**, 1; R. W. Pekala and L. W. Hrubesh, eds., *J. Non-Cryst. Solids*, 1995, **186**, 435; J. Phalippou and R. Vacher, eds., *J. Non-Cryst. Solids*, 1998, **225**, 1.
7 S. S. Kistler, *Nature*, 1931, **127**, 741; S. S. Kistler, *J. Phys. Chem.*, 1934, **38**, 52.
8 S. S. Kistler, S. Swann and E. G. Appel, *Ind. Eng. Chem.*, 1934, **26**, 388.
9 S. S. Kistler and S. A. G. Caldwell, *Ind. Eng. Chem.*, 1934, **26**, 658.
10 G. A. Nicolaon and S. J. Teichner, *Bull. Soc. Chim. Fr.*, 1968, **5**, 1906.
11 C. J. Brinker and G. W. Scherer, *Sol–Gel Science: The Physics and Chemistry of Sol–Gel Processing*, Academic Press, San Diego, 1990.
12 J. Livage, M. Henry and C. Sanchez, *Prog. Solid State Chem.*, 1988, **18**, 259.
13 D. M. Schleich, *Solid State Ionics*, 1994, **70/71**, 407.
14 D. Segal, *J. Mater. Chem.*, 1997, **7**, 1297.
15 G. M. Pajonk, *Appl. Catal.*, 1991, **72**, 217.
16 J. Fricke and A. Emmerling, *J. Am. Ceram. Soc.*, 1992, **75**, 2027.
17 M. Schneider and A. Baiker, *Catal. Rev. Sci. Eng.*, 1995, **37**, 515; M. Schneider and A. Baiker, *Catal. Today*, 1997, **35**, 339.
18 N. Hüsing and U. Schubert, *Angew. Chem., Int. Ed.*, 1998, **37**, 22.
19 R. C. Mehrota, *J. Non-Cryst. Solids*, 1988, **100**, 1.
20 C. Sanchez, J. Livage, M. Henry and F. Babonneau, *J. Non-Cryst. Solids*, 1988, **100**, 65.
21 F. Ribot, P. Toledano and C. Sanchez, *Chem. Mater.*, 1991, **3**, 759.
22 G. W. Scherer, *J. Non-Cryst. Solids*, 1987, **92**, 375.
23 The bulk density of low density materials represents the mass of the gel network per unit volume occupied by the network (which includes the volume occupied by pores) and is not the density of the fully dense solid.
24 The quantitative limit to what is and is not an aerogel is not rigorously defined. The pore volume of materials deemed aerogels can range from $>99\%$ to $\sim 70\%$.
25 P. H. Tewari, A. J. Hunt and K. D. Lofftus, *Mater. Lett.*, 1985, **3**, 363.
26 P. J. Lea and S. A. Ramjohn, *Microscopy Acta*, 1980, **83**, 291.
27 S. S. Prakash, C. J. Brinker, A. J. Hurd and S. M. Rao, *Nature*, 1995, **374**, 439; S. S. Prakash, C. J. Brinker and A. J. Hurd, *J. Non-Cryst. Solids*, 1995, **190**, 264.
28 D. M. Smith, D. Stein, J. M. Anderson and W. Ackerman, *J. Non-Cryst. Solids*, 1995, **186**, 104.
29 T. Gerber, *J. Sol–Gel Sci. Technol.*, 1998, **13**, 323.
30 S. Hæreid, J. Anderson, M.-A. Einarsrud, D. W. Hua and D. M. Smith, *J. Non-Cryst. Solids*, 1995, **185**, 221.
31 S. Hæreid, M. Dahle, S. Lima and M.-A. Einarsrud, *J. Sol–Gel Sci. Technol.*, 1994, **3**, 199; S. Hæreid, M. Dahle, S. Lima and M.-A. Einarsrud, *J. Non-Cryst. Solids*, 1995, **186**, 96; M.-A. Einarsrud, M. B. Kirkedelen, E. Nilsen, K. Mortensen and J. Samseth, *J. Non-Cryst. Solids*, 1998, **231**, 10.
32 S. Hæreid, E. Nilsen and M.-A. Einarsrud, *J. Non-Cryst. Solids*, 1996, **204**, 228.
33 S. Dai, Y. H. Ju, H. J. Gao, J. S. Lin, S. J. Pennycook and C. E. Barnes, *Chem. Commun.*, 2000, 243.
34 B. I. Lee and K. T. Chou, *Mater. Lett.*, 1992, **14**, 112.
35 J. H. Harreld, W. Dong and B. Dunn, *Mater. Res. Bull.*, 1998, **33**, 561.
36 W. Dong, D. R. Rolison and B. Dunn, *Electrochem. Solid State Lett.*, 2000, **3**, 457.
37 S. Passerini, F. Coustier, M. Giorgetti and W. H. Smyrl, *Extended Abstracts of the 196th Electrochemical Society Meeting*, PV-2, 1999, Electrochemical Society, Pennington, NJ, no. 291; S. Passerini, F. Coustier, M. Giorgetti and W. H. Smyrl, *Electrochem. Solid State Lett.*, 1999, **2**, 483.
38 J. W. Long, K. E. Swider and D. R. Rolison, *Extended Abstracts of the 196th Electrochemical Society Meeting*, PV-2, 1999, Electrochemical Society, Pennington, NJ, no. 190; J. W. Long, K. E. Swider, R. M. Stroud and D. R. Rolison, *Electrochem. Solid State Lett.*, 2000, **3**, 453.
39 D. W. Breck, *Zeolite Molecular Sieves*, Wiley, New York, 1974.
40 E. I. Ko, *Chemtech*, 1993, **23**, 31.
41 See for example: *Catalyst Handbook*, 2nd edn., ed. M. V. Twigg, Manson Publishing, London, 1996, ch. 4–10; J. M. Thomas and W. J. Thomas, *Principles and Practice of Heterogeneous Catalysis*, VCH, Weinheim, 1997, ch. 8.
42 H. D. Foster and D. B. Keyes, *Ind. Eng. Chem.*, 1937, **29**, 1254.
43 J. N. Armor, E. J. Carlson and P. M. Zambri, *Appl. Catal.*, 1985, **19**, 339.
44 G. A. Somorjai, *Surf. Sci.*, 1994, **299/300**, 849.
45 F. Blanchard, J. P. Reymond, B. Pommier and S. J. Teichner, *J. Mol. Catal.*, 1982, **17**, 171.
46 N. Sun and K. J. Klabunde, *J. Catal.*, 1999, **185**, 506.
47 J. G. Weissman, E. I. Ko and S. Kaytal, *Appl. Catal. A*, 1993, **94**, 45.
48 J. Cross, R. Goswin, R. Gerlach and J. Fricke, *Rev. Phys. Appl.*, 1989, **24**, C4–185.
49 J. Phalippou, T. Woignier and M. Prassas, *J. Mater. Sci.*, 1990, **25**, 3111.
50 T. Woignier, J. Phalippou and M. Prassas, *J. Mater. Sci.*, 1990, **25**, 3118.
51 J. V. Ryan, A. D. Berry, M. L. Anderson, J. W. Long, R. M. Stroud, V. M. Cepak, V. M. Browning, D. R. Rolison and C. I. Merzbacher, *Nature*, 2000, **406**, 169.
52 K. J. Klabunde, J. Start, O. Koper, C. Mohs, D. G. Park, S. Decker, Y. Jiang, I. Lagadic and D. Zhang, *J. Phys. Chem.*, 1996, **100**, 12142.
53 O. Koper and K. J. Klabunde, *Chem. Mater.*, 1993, **5**, 500.
54 O. B. Koper, E. A. Wovchko, J. A. Glass Jr., J. T. Yates Jr. and K. J. Klabunde, *Langmuir*, 1995, **11**, 2054.
55 O. B. Koper, I. Lagadic, A. Volodin and K. J. Klabunde, *Chem. Mater.*, 1997, **9**, 2468.
56 E. M. Lucas and K. J. Klabunde, *Nanostruct. Mater.*, 1999, **12**, 179.
57 Y.-X. Li and K. J. Klabunde, *Langmuir*, 1991, **7**, 1388; Y.-X. Li, J. R. Schlup and K. J. Klabunde, *Langmuir*, 1991, **7**, 1394.
58 E. M. Lucas and K. J. Klabunde, manuscript in preparation.
59 Y. Jiang, S. Decker, C. Mohs and K. J. Klabunde, *J. Catal.*, 1998, **180**, 24.
60 L. L. Hench and J. K. West, *Chem. Rev.*, 1990, **90**, 33.
61 How controlled are pores sizes in aerogels? The size distribution of the pores and their average sizes in aerogels can be tuned and shifted by control of the sol–gel chemistry and processing. The

degree of control is not, however, as fine as that achieved with surfactant-templated mesoporous silicates and other oxides.[62]
62 U. Ciesla and F. Schüth, *Microporous Mesoporous Mater.*, 1999, **27**, 131.
63 Silica aerogels are also the best thermal insulators off the planet—they were used to insulate the Martian rover, Sojourner (see http://mars.jpl.nasa.gov/ for background and updates on this mission and the plans proposed for a second Mars rover in 2003).
64 J. Fricke and A. Emmerling, in *Chemical Processing of Advanced Materials*, eds. L. L. Hench and J. K. West, Wiley, New York, 1992, pp. 3–17.
65 See for example: A. J. Hunt and K. D. Loftus, *Adv. Sol. Energy Technol.*, 1988, **4**, 3146.
66 J. Fricke, *J. Non-Cryst. Solids*, 1990, **121**, 188.
67 D. M. Smith, W. C. Ackerman, R. Roth, A. Zimmerman and F. Schwertferger, *Mater. Res. Soc. Symp. Proc.*, 1996, **431**, 291.
68 J. Fricke and T. Tillotson, *Thin Solid Films*, 1997, **297**, 212.
69 J. Fricke and G. Reichnauer, *Mater. Res. Soc. Symp. Proc.*, 1986, **73**, 775.
70 M. Cantin, M. Casse, L. Koch, R. Jouan, P. Mestran, D. Roussel, F. Bonnin, J. Moutel and S. J. Teichner, *Nucl. Instrum. Meth.*, 1974, **118**, 177.
71 J. Fricke, *Spektrum der Wissenschaft*, 1988, **7**, 60; M. Bockhorst, K. Heinloth, G. M. Pajonk, R. Begag and E. Elaloui, *J. Non-Cryst. Solids*, 1995, **186**, 388.
72 M. H. W. Chan, K. I. Blum, S. Q. Murphy, G. K. S. Wong and J. D. Reppy, *Phys. Rev. Lett.*, 1988, **61**, 1950; G. K. S. Wong, P. A. Crowell, H. A. Cho and J. D. Reppy, *Phys. Rev. B*, 1993, **48**, 3558.
73 J. V. Porto and J. M. Parpia, *Phys. Rev. Lett.*, 1995, **74**, 4667; A. Golov, J. V. Porto and J. M. Parpia, *J. Low Temp. Phys.*, 1998, **113**, 329, and references therein.
74 P. Tsou, *J. Non-Cryst. Solids*, 1995, **186**, 415.
75 For up-to-the-minute information on the "Stardust" mission check http://stardust.jpl.nasa.gov/ and for further detail on NASA's use of aerogels to capture micrometeorites check http://stardust.jpl.nasa.gov/spacecraft/aerogel.html
76 D. M. Smith, J. Anderson, C. C. Cho, G. P. Johnston and S. P. Jeng, *Mater. Res. Soc. Symp. Proc.*, 1995, **381**, 261.
77 See, for example, *MRS Bull.*, issue on Low Dielectric Constant Materials, October, 1997.
78 The National Technology Roadmap for Semiconductors (Semiconductor Industry Association, San Jose, 1997); the international status of the roadmap can be monitored at: http://public.itrs.net/
79 R. J. Ayen and P. A. Iacobucci, *Rev. Chem. Eng.*, 1988, **5**, 157.
80 A. J. Hunt and W. Cao, *Mater. Res. Soc. Symp. Proc.*, 1994, **346**, 451.
81 J. M. Miller, B. Dunn, T. D. Tran and R. Pekala, *J. Electrochem. Soc.*, 1997, **144**, L309; J. M. Miller and B. Dunn, *Langmuir*, 1999, **15**, 799.
82 C. I. Merzbacher, J. G. Barker, K. E. Swider, J. V. Ryan, R. A. Bernstein and D. R. Rolison, *J. Non-Cryst. Solids*, 1998, **225**, 234.
83 C. I. Merzbacher, J. G. Barker, J. V. Ryan, R. A. Bernstein, J. W. Long and D. R. Rolison, *Nanostruct. Mater.*, 1999, **12**, 551.
84 N. Hüsing and U. Schubert, *J. Sol–Gel Sci. Technol.*, 1997, **8**, 807, and references therein.
85 P. Judeinstein and C. Sanchez, *J. Mater. Chem.*, 1996, **6**, 511.
86 C. I. Merzbacher, J. G. Barker, K. E. Swider and D. R. Rolison, *J. Non-Cryst. Solids*, 1998, **224**, 92.
87 Refilling the aerogel's pores with water, prior to the neutron scattering experiment, was done either in stages (*e.g.*, by first filling the micropores by vapor-phase equilibration with the appropriate pure or contrast-matched fluid before immersion into the liquid) or by direct immersion in the pure or contrast-matched liquid. Similar results were obtained with both approaches.[86]
88 C. I. Merzbacher, J. G. Barker, K. E. Swider and D. R. Rolison, *Adv. Colloid Interface Sci.*, 1998, **76–77**, 57.
89 B. Scrosati and C. Vincent, *Modern Batteries*, 2nd edn., Arnold, London, 1997.
90 K. B. Oldham and J. C. Myland, *Fundamentals of Electrochemical Science*, Academic, San Diego, 1994, pp. 11–12.
91 R. Richards, W. Li, S. Decker, C. Davidson, O. Koper, V. Zaikovski, A. Volodin, T. Rieker and K. J. Klabunde, *J. Am. Chem. Soc.*, 2000, **122**, 4921.
92 R. W. Pekala, *J. Mater. Sci.*, 1989, **24**, 3221; R. W. Pekala and D. W. Schaefer, *Macromolecules*, 1993, **26**, 5487.
93 S. T. Mayer, R. W. Pekala and J. L. Kaschmitter, *J. Electrochem. Soc.*, 1993, **140**, 446.
94 J. C. Farmer, D. V. Fix, G. V. Mack, R. W. Pekala and J. F. Poco, *J. Electrochem. Soc.*, 1996, **143**, 159.
95 G. M. Pajonk, A. V. Rao, N. Pinto, F. Ehrburger-Dolle and M. G. Gil, *Stud. Surf. Sci. Catal.*, 1998, **118**, 167.
96 Emphasis must be placed on the word "gels": metal oxide films can be created by spin- or dip-coating viscous media containing MOx precursors, which are then sintered and densified, so that a pre-formed network morphology need not be created before the drying step; aerogels, however, must have network-formed wet gels before either SCD or ambient-pressure drying is performed. Network formation requires control over the polycondensation component of sol–gel chemistry.[18]
97 J. Livage, *Chem. Mater.*, 1991, **3**, 578.
98 R. Baddour, J. P. Pereira-Ramos, R. Messina and J. Perichon, *J. Electroanal. Chem.*, 1991, **314**, 81; B. Araki, C. Mailhe, N. Baffier, J. Livage and J. Vedel, *Solid State Ionics*, 1983, **9/10**, 439.
99 K. West, B. Zachau-Christiansen, T. Jacobsen and S. Skaarup, *Electrochim. Acta*, 1993, **38**, 1215.
100 T. Miura, E. Sugiura, T. Kishii and T. Nagai, *Denki Kagaku*, 1988, **56**, 413; T. Miura, S. Kunihiro, Y. Muranushi and T. Nagai, *Denki Kagaku*, 1989, **57**, 393.
101 H.-K. Park and W. H. Smyrl, *J. Electrochem. Soc.*, 1994, **141**, L25; H.-K. Park, W. H. Smyrl and M. D. Ward, *J. Electrochem. Soc.*, 1995, **142**, 1068.
102 H. Hirashima and K. Sudoh, *J. Non-Cryst. Solids*, 1992, **145**, 51.
103 K. Sudoh and H. Hirashima, *J. Non-Cryst. Solids*, 1992, **147/148**, 386.
104 F. Chaput, B. Dunn, P. Fuqua and K. Salloux, *J. Non-Cryst. Solids*, 1995, **188**, 11.
105 D. B. Le, S. Passerini, A. L. Tipton, B. B. Owens and W. H. Smyrl, *J. Electrochem. Soc.*, 1995, **142**, L102.
106 D. B. Le, S. Passerini, J. Guo, J. Ressler, B. B. Owens and W. H. Smyrl, *J. Electrochem. Soc.*, 1996, **143**, 2099.
107 B. Katz, W. Liu, K. Salloux, F. Chaput, B. Dunn and G. C. Farrington, *Mater. Res. Soc. Symp. Proc.*, 1995, **369**, 211.
108 G. W. Scherer, *J. Colloid Interface Sci.*, 1998, **202**, 399.
109 K. Salloux, F. Chaput, H. P. Wong, B. Dunn and M. W. Breiter, *J. Electrochem. Soc.*, 1995, **142**, L191.
110 W. Weppner and R. A. Huggins, *J. Electrochem. Soc.*, 1977, **124**, 1569; W. Weppner and R. A. Huggins, *Annu. Rev. Mater. Sci.*, 1978, **8**, 269; W. Weppner and R. A. Huggins, *Int. Met. Rev.*, 1981, **5**, 253.
111 S. Passerini, D. B. Le, W. H. Smyrl, M. Berrettoni, R. Tossici, R. Marassi and M. Giorgetti, *Solid State Ionics*, 1997, **104**, 195.
112 *C*/*x* is the charge rate of a battery;[113] *e.g.*, to charge a 120 A h battery in 4 h (a *C*/4 rate) requires applying a current of 30 A.
113 *Handbook of Batteries and Fuel Cells*, ed. D. Linden, Mc-Graw Hill, New York, 1984, p. A-4.
114 F. Coustier, S. Passerini and W. H. Smyrl, *J. Electrochem. Soc.*, 1998, **145**, L73; F. Coustier, J.-M. Lee, S. Passerini and W. H. Smyrl, *Solid State Ionics*, 1999, **116**, 279.
115 D. Fauteux and B. Dunn, unpublished results.
116 S. Passerini, W. H. Smyrl, M. Berrettoni, R. Tossici, M. Rosolen, R. Marassi and F. Decker, *Solid State Ionics*, 1996, **90**, 5.
117 M. Giogetti, S. Passerini, W. H. Smyrl, S. Mukerjee, X. Q. Yang and J. McBreen, *J. Electrochem. Soc.*, 1999, **146**, 2387.
118 J. Wong, F. W. Lytle, R. P. Messmer and D. H. Maylotte, *Phys. Rev. B*, 1984, **30**, 5596.
119 H. P. Wong, B. C. Dave, F. Leroux, J. Harreld, B. Dunn and L. F. Nazar, *J. Mater. Chem.*, 1998, **8**, 1019.
120 D. B. Le, S. Passerini, F. Coustier, J. Guo, T. Soderstrom, B. B. Owens and W. H. Smyrl, *Chem. Mater.*, 1998, **10**, 682.
121 B. Yebka and C. Julien, *Mater. Res. Soc. Symp. Proc.*, 1995, **369**, 119; J. P. Pereira-Ramos, N. Kumagai and N. Kumagai, *J. Power Sources*, 1995, **56**, 87.
122 S. Mukerjee, S. J. Lee, E. A. Ticianelli, J. McBreen, B. N. Grgur, N. M. Markovic, P. N. Ross, J. R. Giallombardo and E. S. DeCastro, *Electrochem. Solid State Lett.*, 1999, **2**, 12; H. Zhang, Y. Wang, E. Rosim Fachini and C. R. Cabrera, *Electrochem. Solid State Lett.*, 1999, **2**, 437.
123 W. Dong and B. Dunn, *J. Mater. Chem.*, 1998, **8**, 665.
124 W. Dong and B. Dunn, *J. Non-Cryst. Solids*, 1998, **225**, 135.
125 M. M. Thackeray, *Prog. Solid State Chem.*, 1997, **25**, 1.
126 W. I. F. David, M. M. Thackeray, L. A. de Picciotto and J. B. Goodenough, *J. Solid State Chem.*, 1987, **67**, 316; T. Ohzuku, M. Kitagawa and T. Hirai, *J. Electrochem. Soc.*, 1990, **137**, 769.
127 M. Winter, J. O. Besenhard, M. E. Spahr and P. Novák, *Adv. Mater.*, 1998, **10**, 725.

128 S. L. Brock, N. G. Duan, Z. R. Tian, O. Giraldo, H. Zhou and S. L. Suib, *Chem. Mater.*, 1998, **10**, 2619.
129 A. Manthiram and J. Kim, *Chem. Mater.*, 1998, **10**, 2895.
130 J. J. Xu, A. J. Kinser, B. B. Owens and W. H. Smyrl, *Electrochem. Solid State Lett.*, 1998, **1**, 1; J. J. Zu, B. B. Owens and W. H. Smyrl, *Extended Abstracts of the 196th Electrochemical Society Meeting*, PV-2, 1999, Electrochemical Society, Pennington, NJ, no. 296.
131 F. Leroux and L. F. Nazar, *Solid State Ionics*, 1997, **100**, 103.
132 J. W. Long, R. M. Stroud and D. R. Rolison, *J. Non-Cryst. Solids*, 2001, in press.
133 J. Kim and A. Manthiram, *Nature*, 1997, **390**, 265; J. Kim and A. Manthiram, *Electrochem. Solid State Lett.*, 1999, **2**, 55.
134 S. Bach, M. Henry, N. Baffier and J. Livage, *J. Solid State Chem.*, 1990, **88**, 325.
135 S. Trasatti, *Electrochim. Acta*, 1991, **36**, 225, and references therein.
136 H. Schafer, G. Schneidereit and W. Gerhardt, *Z. Anorg. Allg. Chem.*, 1963, **319**, 372.
137 A. Mills, C. Lawrence and R. Enos, *J. Chem. Soc., Chem. Commun.*, 1984, 1436.
138 S. Ardizzone, A. Carugati, G. Lodi and S. Trasatti, *J. Electrochem. Soc.*, 1982, **129**, 1689.
139 J. P. Zheng, P. J. Cygan and T. R. Jow, *J. Electrochem. Soc.*, 1995, **142**, 2699.
140 J. W. Long, K. E. Swider, C. I. Merzbacher and D. R. Rolison, *Langmuir*, 1999, **15**, 780.
141 K. E. Swider, C. I. Merzbacher, P. L. Hagans and D. R. Rolison, *J. Non-Cryst. Solids*, 1998, **225**, 348.
142 Yu. E. Roginskaya, B. Sh. Galyamov, V. M. Lebedev, I. D. Belova and Yu.N. Venevtsev, *Russ. J. Inorg. Chem.*, 1977, **22**, 273; M. Valigi and D. Gazzoli, *Z. Phys. Chem. Neue Folge*, 1981, **125**, 89.
143 G. Dagan and M. Tomkiewicz, *J. Phys. Chem.*, 1993, **97**, 12651.
144 The surfaces of many oxide-based electrodes (including ion-selective materials such as pH-sensitive glass) are described as a solid-state reservoir (at standard state) over which a nanoscale, hydrated (gel-like) layer intermediates the ionic (*i.e.*, electrical) communication between the liquid electrolyte and the bulk solid state of the oxide.[145]
145 W. E. Morf, *The Principles of Ion-Selective Electrodes and Membrane Transport, Studies in Analytical Chemistry, Vol. 2*, Elsevier, Amsterdam, 1981, pp. 362–363.
146 D. R. Rolison, P. L. Hagans, K. E. Swider and J. W. Long, *Langmuir*, 1999, **15**, 774.
147 D. A. McKeown, P. L. Hagans, L. P. L. Carette, A. E. Russell, K. E. Swider and D. R. Rolison, *J. Phys. Chem. B*, 1999, **103**, 4825.
148 F. A. Kröger, *The Chemistry of Imperfect Crystals*, Vol. 2, Elsevier, New York, 1974, p. 14.
149 L. F. Nazar, in *Access in Nanoporous Materials*, ed. T. Pinnavaia and M. Thorpe, Plenum Press, New York, 1995, pp. 405–427.
150 F. Leroux, G. Goward, W. P. Power and L. F. Nazar, *J. Electrochem. Soc.*, 1997, **144**, 3886.
151 F. Huguenin, M. T. do Prado Gambardella, R. M. Torresi, S. I. Córdoba de Torresi and D. A. Buttry, *J. Electrochem. Soc.*, 2000, **147**, 2437.
152 B. C. Dave, B. Dunn, F. Leroux, L. F. Nazar and H. P. Wong, *Mater. Res. Soc. Symp. Proc.*, 1996, **435**, 611.
153 J. Harreld, H. P. Wong, B. C. Dave, B. Dunn and L. F. Nazar, *J. Non-Cryst. Solids*, 1998, **225**, 319.
154 J. H. Harreld, B. Dunn and L. F. Nazar, *Int. J. Inorg. Mater.*, 1999, **1**, 135.
155 W. Dong and B. Dunn, *Mater. Res. Soc. Symp. Proc.*, 1999, **576**, 269.
156 T. A. Kerr, H. Wu and L. F. Nazar, *Chem. Mater.*, 1996, **8**, 2005.
157 D. Belanger, G. Laperriere and L. Gravel, *J. Electrochem. Soc.*, 1990, **137**, 365.
158 C. A. Morris, M. L. Anderson, R. M. Stroud, C. I. Merzbacher and D. R. Rolison, *Science*, 1999, **284**, 622.
159 R. Zallen, *The Physics of Amorphous Materials*, Wiley, New York, 1998, ch. 4.
160 Aerogels have a dimensionality that is less than three, but greater than two, as confirmed by X-ray and neutron-scattering measurements.[161]
161 D. W. Schaefer and K. D. Keefer, *Phys. Rev. Lett.*, 1986, **56**, 2199.
162 V. M. Cepak, J. V. Ryan, M. L. Anderson, C. I. Merzbacher and D. R. Rolison, Naval Research Laboratory, unpublished results.
163 J. J. Pietron and D. R. Rolison, *J. Non-Cryst. Solids*, 2001, in press.
164 For example, see: *Photocatalysis: Fundamentals and Applications*, ed. D. F. Ollis, E. Pelizzetti and N. Serpone, Wiley, New York, 1989; M. R. Hoffmann, S. T. Martin, W. Choi and D. W. Bahnemann, *Chem. Rev.*, 1995, **95**, 69.
165 For example, see: B. O'Regan and M. Grätzel, *Nature*, 1991, **353**, 737; R. Argazzi, C. A. Bignozzi, T. A. Heimer, F. N. Castellano and G. J. Meyer, *J. Am. Chem. Soc.*, 1995, **117**, 11815.
166 S. A. Walker, P. A. Christensen, K. E. Shaw and G. M. Walker, *J. Electroanal. Chem.*, 1995, **393**, 137.
167 G. E. Pike and C. H. Seager, *J. Appl. Phys.*, 1977, **48**, 5152.
168 S. Yamamichi, P. Y. Lesaicherre, H. Yamaguchi, K. Takemura, S. Sone, H. Yabuta, K. Sato, T. Tamura, K. Nakajima, S. Ohnishi, K. Tokashiki, Y. Hayashi, Y. Kato, Y. Miyasaka, M. Yoshida and H. Ono, *IEEE Trans. Elec. Dev.*, 1997, **44**, 1076.
169 J. Koresh and A. Soffer, *J. Electrochem. Soc.*, 1977, **124**, 1379.
170 D. Pletcher and F. C. Walsh, *Industrial Electrochemistry*, 2nd edn., Chapman & Hall, London, 1993; E. Heitz and G. Kreysa, *Principles of Electrochemical Engineering*, VCH, Weinheim, Germany, 1986.
171 J. S. Newman, *Electrochemical Systems*, 2nd edn., Prentice Hall, Englewood Cliffs, NJ, 1991, ch. 22.
172 A. J. Bard and L. R. Faulkner, *Electrochemical Methods—Fundamentals and Applications*, Wiley, New York, 1980, pp. 26–34.
173 D. Geldart, *Powder Technol.*, 1973, **7**, 285.
174 J. Chaouki, C. Chavarie, D. Klvana and G. Pajonk, *Powder Technol.*, 1985, **43**, 117; H. Li, R. Legros, C. M. H. Brereton, J. R. Grace and J. Chaouki, *Powder Technol.*, 1990, **60**, 121.
175 C. A. Morris and D. R. Rolison, manuscript in preparation.
176 N. A. Surridge, J. C. Jernigan, E. F. Dalton, R. P. Buck, M. Watanabe, H. Zhang, M. Pinkerton, T. T. Wooster, M. L. Longmire, J. S. Facci and R. W. Murray, *Faraday Discuss. Chem. Soc.*, 1989, **88**, 1.
177 T. Pajkossy, *J. Electroanal. Chem.*, 1991, **300**, 1.
178 A. Harrison, *Fractals in Chemistry*, Oxford University Press, Oxford, England, 1996.
179 T. Pajkossy and L. Nyikos, *Electrochim. Acta*, 1989, **34**, 171.
180 A. J. Jarzębski, J. Lorenc and L. Pająk, *Langmuir*, 1997, **13**, 1280.
181 N. Leventis, I. Elder, D. R. Rolison, M. L. Anderson and C. I. Merzbacher, *Chem. Mater.*, 1999, **11**, 2837.
182 If chemically modified aerogels are prepared as thin films, as Hrubesh *et al.* have shown is feasible with pure silica,[183] the response of a 10 μm thick, fluorophore-modified aerogel film would fall in the millisecond regime for gas-phase analytes.
183 L. Hrubesh and J. F. Poco, *J. Non-Cryst. Solids*, 1995, **188**, 46.
184 B. E. Conway, *J. Electrochem. Soc.*, 1991, **138**, 1539.
185 M. Broussely, P. Biensan and B. Simon, *Electrochim. Acta*, 1999, **45**, 3.
186 B. B. Owens, S. Passerini and W. H. Smyrl, *Electrochim. Acta*, 1999, **45**, 215.
187 J. W. Long and D. R. Rolison in *New Directions in Electroanalytical Chemistry II*, ed. J. Leddy, P. Vanýsek and M. D. Porter, PV99-5, Electrochemical Society, Pennington, NJ, 1999, pp. 125–131.
188 J. W. Long and D. R. Rolison, manuscript in preparation.
189 K. West, in *Intercalation Chemistry*, ed. M. S. Whittingham and A. J. Jacobson, Academic Press, San Diego, 1982, pp. 447–477.
190 P. G. Bruce, *Chem. Commun.*, 1997, 1817.
191 C. R. Horne, U. Bergmann, J. Kim, K. A. Striebel, A. Manthiram, S. P. Cramer and E. J. Cairns, *J. Electrochem. Soc.*, 2000, **147**, 395.
192 J.-C. Badot and N. Baffier, *J. Mater. Chem.*, 1992, **2**, 1167.
193 K. Hermann, M. Witko and R. Druzinic, *Faraday Discuss.*, 1999, **114**, 53.
194 P. Ruetschi, *J. Electrochem. Soc.*, 1984, **131**, 2737.
195 P. Ruetschi, *J. Electrochem. Soc.*, 1988, **135**, 2657.
196 P. Ruetschi and R. Giovanoli, *J. Electrochem. Soc.*, 1988, **135**, 2663.
197 P. Vanýsek, *Electrochim. Acta*, 1995, **40**, 2841; H. H. Girault and D. J. Schriffin, in *Electroanalytical Chemistry*, ed. A. J. Bard, vol. 15, Marcel Dekker, New York, 1989, pp. 1–141.
198 H. S. White, J. D. Peterson, Q. Z. Cui and K. J. Stevenson, *J. Phys. Chem. B*, 1998, **102**, 2930.
199 K. E. Swider-Lyons, C. T. Love and D. R. Rolison, manuscript in preparation.
200 G. B. Appetecchi and B. Scrosati, *Electrochim. Acta*, 1998, **43**, 1105.
201 W. H. Meyer, *Adv. Mater.*, 1998, **10**, 439.
202 J. Eckert, G. D. Stucky and A. K. Cheetham, *Mater. Res. Bull.*, 1999, **24**, 31.
203 D. R. Rolison and C. A. Bessel, *Acc. Chem. Res.*, 2000, **33**, 737.